

Protein Kinase CK2 Acts as a Molecular Brake to Control NADPH Oxidase 1 Activation and Colon Inflammation

Dan Liu, Jean-Claude Marie, Anne-Laure Pelletier, Zhuoyao Song, Marwa Ben Khemis, Kaouthar Boudiaf, Coralie Pintard, Thibaut Leger, Samuel Terrier, Guillaume Chevreux, et al.

▶ **To cite this version:**

Dan Liu, Jean-Claude Marie, Anne-Laure Pelletier, Zhuoyao Song, Marwa Ben Khemis, et al.. Protein Kinase CK2 Acts as a Molecular Brake to Control NADPH Oxidase 1 Activation and Colon Inflammation. Cellular and Molecular Gastroenterology and Hepatology, 2022, 13 (4), pp.1073 - 1093. 10.1016/j.jcmgh.2022.01.003 . anses-03664190

HAL Id: anses-03664190

https://anses.hal.science/anses-03664190

Submitted on 10 May 2022

HAL is a multi-disciplinary open access archive for the deposit and dissemination of scientific research documents, whether they are published or not. The documents may come from teaching and research institutions in France or abroad, or from public or private research centers.

L'archive ouverte pluridisciplinaire **HAL**, est destinée au dépôt et à la diffusion de documents scientifiques de niveau recherche, publiés ou non, émanant des établissements d'enseignement et de recherche français ou étrangers, des laboratoires publics ou privés.



Distributed under a Creative Commons Attribution - NonCommercial - NoDerivatives 4.0 International License

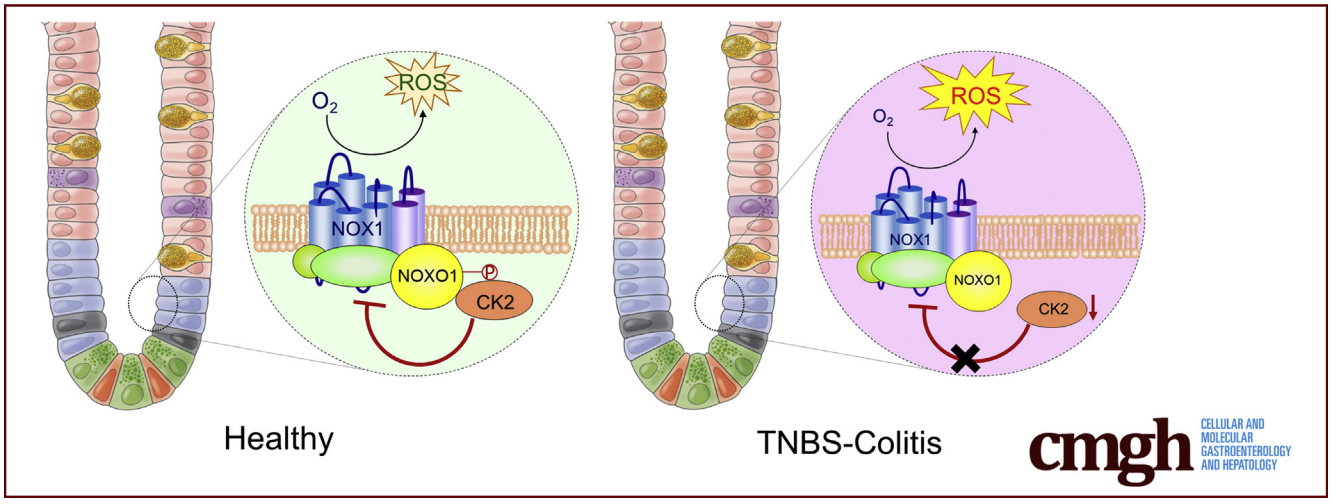
cmgh
CELLULAR AND MOLECULAR GASTROENTEROLOGY AND HEPATOLOGY

ORIGINAL RESEARCH

Protein Kinase CK2 Acts as a Molecular Brake to Control NADPH Oxidase 1 Activation and Colon Inflammation

Dan Liu,[1] Jean-Claude Marie,[1] Anne-Laure Pelletier,[2] Zhuoyao Song,[1] Marwa Ben-Khemis,[1] Kaouthar Boudiaf,[1] Coralie Pintard,[1] Thibaut Leger,[3,4] Samuel Terrier,[3] Guillaume Chevreux,[3] Jamel El-Benna,[1] and Pham My-Chan Dang[1]

[1]*INSERM U1149, CNRS ERL8252, Centre de Recherche sur l'Inflammation, Université de Paris, Laboratoire d'Excellence Inflamex, Faculté de Médecine, Site Xavier Bichat, Paris;* [2]*Service d'Hépato-Gastroentérologie et Cancérologie Digestive, Hôpital Bichat–Claude Bernard, Paris;* [3]*Proteoseine@IJM, Institut Jacques Monod - Université Paris, Paris, France; and* [4]*Toxicology of Contaminants Unit, Fougères Laboratory, French Agency for Food, Environmental and Occupational Health & Safety (ANSES), 35306 Fougères CEDEX, France*



SUMMARY

Protein kinase CK2 is a major partner of NOXO1 in human colon epithelial cells; it directly binds and phosphorylates NOXO1 to decrease ROS generation by NOX1. In TNBS-induced colitis, the decrease in CK2 activity results in increased ROS production, thereby exacerbating inflammation.

BACKGROUND & AIMS: NADPH oxidase 1 (NOX1) has emerged as a prime regulator of intestinal mucosa immunity and homeostasis. Dysregulation of NOX1 may cause inflammatory bowel disease (IBD). It is not clear how NOX1 is regulated *in vivo* under inflammatory conditions. We studied the role of CK2 in this process.

METHODS: The NOX1 organizer subunit, NADPH oxidase organizer 1 (NOXO1), was immunoprecipitated from cytokine-treated colon epithelial cells, and bound proteins were identified by mass spectrometry analysis. Sites on NOXO1 phosphorylated by CK2 were identified by nanoscale liquid chromatography coupled to tandem mass spectrometry. NOX1 activity was determined in colon epithelial cells and colonoids in the presence or absence of CX-4945, a CK2 specific inhibitor. Acute colitis was induced by administration of trinitrobenzenesulfonic acid in mice treated or not with CX-4945. Colon tissues were analyzed by histologic examination, quantitative polymerase chain reaction, and Western blots. CK2 activity, markers of inflammation, and oxidative stress were assessed.

RESULTS: We identified CK2 as a major partner of NOXO1 in colon epithelial cells under inflammatory conditions. CK2 directly binds NOXO1 at the C-terminus containing the Phox homology domain and phosphorylates NOXO1 on several sites. CX-4945 increased ROS generation by NOX1 in human colon epithelial cells and organoids. Strikingly, CK2 activity was reduced in trinitrobenzenesulfonic acid–induced acute colitis, and CX-4945 exacerbated colitis inflammation as shown by increased levels of CXCL1, ROS generation, lipid peroxidation, and colon damage.

CONCLUSIONS: The ubiquitous protein kinase CK2 limits NOX1 activity via NOXO1 binding and phosphorylation in colonic epithelial cells and lessens experimental colitis. Loss of CK2 activity during acute colitis results in excessive ROS production, contributing to the pathogenesis. Strategies to activate CK2 could be an effective novel therapeutic approach in IBD. *(Cell Mol Gastroenterol Hepatol 2022;13:1073–1093; https://doi.org/10.1016/j.jcmgh.2022.01.003)*

Keywords: NOX1; CK2; ROS; IBD..

The gastrointestinal tract fulfills several physiological functions while undergoing permanent antigenic pressure from various sources of antigens. It must therefore coordinate appropriate immune and inflammatory responses against potential infection and to maintain immune homeostasis.[1] Gastrointestinal epithelial cells, which constitute a physical barrier against commensal or pathogenic microbes, coordinate the immune response by secreting diverse innate immune proteins and inflammatory mediators and producing reactive oxygen species (ROS).[2,3]

In response to inflammatory stimuli, intestinal epithelial cells produce ROS through specialized enzymes called nicotinamide adenine dinucleotide phosphate (NADPH) oxidases (NOXs). The NOXs are multi-subunit enzymatic complexes dedicated to the controlled production of superoxide anion ($O_2^{\circ-}$). This family includes 7 members, NOX 1–5 and dual oxidase 1 and 2 (DUOX1, DUOX2), which have specific tissue expression.[3,4] The intestinal mucosal epithelium expresses NOX1 and DUOX2. DUOX2 is expressed at low level all along the digestive tract epithelium, whereas NOX1 is abundantly expressed in the colon epithelium.[5,6] NOX1 has well-established physiopathologic roles.[3] The NOX1 complex consists of the transmembrane proteins, NOX1 and $p22^{PHOX}$, and the cytosolic proteins, NOX organizer 1 (NOXO1), NOX activator 1 (NOXA1), and Rac1. Four NOXO1 isoforms have been described, but only the β and γ isoforms are expressed in colon epithelial cells and can support NOX1 activity.[3] NOX1, the catalytic core through which electrons are transferred to reduce oxygen, gives its name to the complex. The membrane $p22^{PHOX}$ subunit stabilizes NOX1, whereas NOXO1 and NOXA1 regulate NOX1 activity by organizing the complex assembly and promoting its catalytic activity, respectively. All components are required for the activity of the enzyme.

NOX1-derived ROS are known to contribute to mucosal immune defense and homeostatic functions, including alteration of bacterial capsule formation,[7] control of bacteriostatic protein expression such as lipocalin 2,[8] chemokine synthesis,[9] and epithelium renewal, restitution, and healing.[10] Consistent with these important physiological functions, dysregulation of NOX1 by loss-of-function or excessive activity may cause pathologic conditions in the gastrointestinal tract such as inflammatory bowel disease (IBD), a group of chronic and relapsing disorders comprising Crohn's disease (CD) and ulcerative colitis (UC) that are characterized by severe inflammation of the intestines. *NOX1* gene variants associated with loss of function have been described in human very early-onset IBD[11]; however, overexpression of NOX1 and NOXO1 has also been observed in UC and CD.[8,12]

We and others have shown that NOX1 has a constitutive activity that can be modulated by phosphorylation of NOXA1 and NOXO1. Phosphorylation of NOXA1 by protein kinase A and mitogen-activated protein kinase was shown to decrease NOX1 activity,[13,14] whereas phosphorylation of NOXO1 by protein kinase C (PKC) enhances it.[15,16] Protein kinase CK2, formerly called casein kinase 2, is a serine/threonine-selective kinase with very special features. It is ubiquitously expressed in all eukaryotic organisms, and its activity does not require any post-translational modification or second messengers,[17] making it constitutive, an unusual feature for a kinase. In addition, it is highly pleiotropic with a broad repertoire of substrates, and in accordance, it is involved in a plethora of cellular functions including cell cycle progression, cell survival, transcription, and translation.[18] CK2 is a tetrameric enzyme composed of 2 catalytic subunits (CK2α and/or α'), and 2 regulatory subunits (CK2β). A third catalytic isoform (CK2α3) has been identified but is not well-described. The catalytic subunits of CK2 are active whether the CK2β subunits are present or not. CK2β could act as a scaffold to define substrate specificity.[18] Recently, CK2 has emerged as a regulator of immunity and inflammation in the intestines through several processes, including epithelial cell restitution during inflammation,[19] control of CD4+ T-cell effector function in experimental colitis,[20] and regulation of the tight junction component claudin-2, thus modulating paracellular permeability and impacting immune-mediated experimental colitis.[21]

Here, we report that CK2 acts as a molecular brake via NOXO1 binding and phosphorylation, thereby controlling NOX1 activation and colon inflammation. Furthermore, our study shows that CK2 activity is decreased and ROS production increased in a mouse model of trinitrobenzenesulfonic acid (TNBS)-induced acute colitis, suggesting a potential mechanism for tissue damage in acute colitis and opening a new avenue for treating intestine inflammation in IBD.

Results

CK2 Interacts With NOXO1 in Colon Epithelial Cells Under Inflammatory Conditions Through the N-Terminus Containing the Phox Homology Domain

We recently demonstrated that the combination of the 2 key inflammatory cytokines found in IBD, eg, tumor necrosis factor (TNF) α and interleukin (IL) 17, induces a dramatic up-regulation of NOXO1 expression in colon epithelial cells,

Abbreviations used in this paper: **ANOVA, analysis of variance; BSA, bovine serum albumin; CD, Crohn's disease; CK2, protein kinase CK2; DMSO, dimethyl sulfoxide; DSS, dextran sulfate sodium; IBD, inflammatory bowel disease; IgG, immunoglobulin G; IL17, interleukin 17; IPP, immunoprecipitates; MDA, malondialdehyde; NADPH, reduced nicotinamide adenine dinucleotide phosphate; nanoLC-MS/MS, nanoscale liquid chromatography coupled to tandem mass spectrometry; NBT, nitroblue tetrazolium; NOXA1, NADPH oxidase activator 1; NOX1, NADPH oxidase 1; NOXO1, NADPH oxidase organizer 1; PBS, phosphate-buffered saline; PKC, protein kinase C; PMA, phorbol myristate acetate; PX, Phox homology; ROS, reactive oxygen species; SDS-PAGE, sodium dodecyl sulfate-polyacrylamide gel electrophoresis; SE, standard error of the mean; TBBz, tetrabromobenzimidazole; TNBS, trinitrobenzenesulfonic acid; TNF, tumor necrosis factor; UC, ulcerative colitis; WT, wild-type; XIC, extracted-ion chromatogram.**

Most current article

© 2022 The Authors. Published by Elsevier Inc. on behalf of the AGA Institute. This is an open access article under the CC BY-NC-ND license (http://creativecommons.org/licenses/by-nc-nd/4.0/).

2352-345X
https://doi.org/10.1016/j.jcmgh.2022.01.003

leading to increased ROS production by NOX1.[8] To identify new regulators of NOX1 upon inflammatory conditions, NOXO1 was immunoprecipitated from the human T84 colonic epithelial cell line co-stimulated by TNFα and IL17, and its bound partners were identified by mass spectrometry analysis (Table 1). As expected, NOXO1 was abundantly found in the NOXO1-immunoprecipitates (NOXO1-IPP) but barely present in the control immunoglobulin G (IgG)-immunoprecipitated fraction (IgG-IPP). Not surprisingly, NOX1 subunits (NOXA1, cytochrome b-245 light chain/ $p22^{PHOX}$), known regulators of ROS production such as cytoskeleton proteins (actin, moesin, coronin) and GTP binding proteins (Rho GTPase-activating protein), and redox signaling proteins (thioredoxin, superoxide dismutase, glutathione peroxidase) co-immunoprecipitated with NOXO1 when immunoprecipitation was performed with a NOXO1 antibody, but not or only weakly when using a control IgG antibody (Table 1). Remarkably, all the CK2 subunits (α, α', α3, and β) could be detected unambiguously among the identified proteins, with a high mascot score, large number of peptides matching the protein, and good sequence coverage. None of these CK2 subunits could be detected in the assay immunoprecipitated with control IgG antibody, demonstrating the specific association with NOXO1. Although co-stimulation of T84 epithelial cells with TNFα + IL17 increased NOXO1 expression concomitantly with ROS generation by NOX1,[8] as shown in Figure 1*A* and *B*, it did not change the expression level of CK2α/α' and CK2β; the latter was very weakly expressed (Figure 1*A*). This result suggests a spontaneous interaction between CK2 and NOXO1 after induction of NOXO1 expression by TNFα + IL17. The association between CK2 and NOXO1 was confirmed by Western blotting of the IPP. CK2α/α' was clearly detected in the NOXO1-IPP when cells were co-stimulated by TNFα + IL17 but noticeably at lower level when cells were unstimulated or stimulated with either TNFα or IL17 alone (Figure 1*C* and *D*). No CK2α/α'could be detected in the control IgG-IPP of cells co-stimulated with

Table 1. Proteins Co-Immunoprecipitating With NOXO1 in T84 Cells Stimulated by TNFα (5 ng/mL) + IL17 (50 ng/mL) and Related to NADPH Oxidase or Redox Signaling

					IgG-IPP		NOXO1-IPP	
Accession	Description	MW	Gene	Coverage	Mascot	No. of peptides	Mascot	No. of peptides
NOXs related proteins								
Q8NFA2	NADPH oxidase organizer 1	41,2	NOXO1	66%	62	3	2436	24
Q86UR1	NADPH oxidase activator 1	50,9	NOXA1	13%	—	—	127	4
P13498	Cytochrome b-245 light chain	20,99	CYBA	4%	—	—	32	1
Q9H0H5	Rac GTPase-activating protein 1	70,98	RACGAP1	4%	—	—	73	2
P07237	Protein disulfide-isomerase	87,08	P4HB	34%	218	5	691	15
Cytoskeleton proteins regulating NOXs								
P63261	Actin, cytoplasmic	41,76	ACTG1	66%	672	12	1510	21
P26038	Moesin	67,77	MSN	3%	—	—	49	2
Q9BR76	Coronin-1B	54,2	CORO1B	2%	—	—	43	1
Q9ULV4	Coronin-1C	53,21	CORO1C	8%	36	1	97	3
GTP binding protein								
P85298	Rho GTPase-activating protein 8	53,45	ARHGAP8	24%	—	—	59,15	6
Q13283	Ras GTPase-activating protein-binding protein 1	52,13	G3BP1	24%	—	—	152,36	7
P01111	GTPase NRas	21,21	NRAS	12%	—	—	43,53	2
Redox signaling protein								
P10599	Thioredoxin	11,7	TXN	32%	—	—	59,27	3
Q9H3N1	Thioredoxin-related transmembrane protein 1	31,77	TMX1	15%	—	—	99	4
P04179	Superoxide dismutase [Mn], mitochondrial	24,7	SOD2	29%	52	1	200	6
P00441	Superoxide dismutase [Cu-Zn]	15,92	SOD1	16%	—	—	94	2
P10620	Microsomal glutathione S-transferase 1	15,58	MGST1	10%	—	—	40,43	1
P22352	Glutathione peroxidase 3	25,53	GPX3	7%	—	—	25	1
Casein kinase 2								
P19784	Casein kinase II subunit alpha'	41,18	CSNK2A2	53%	—	—	489	15
P68400	Casein kinase II subunit alpha	45,11	CSNK2A1	44%	—	—	420	12
Q8NEV1	Casein kinase II subunit alpha 3	45,19	CSNK2A3	41%	—	—	405	11
P67870	Casein kinase II subunit beta	24,92	CSNK2B	24%	—	—	143	3

NOTE. Immunoprecipitation of NOXO1 was performed in T84 whole cell lysates. Proteins were trypsin digested in gel, and extracted peptides were analyzed by nanoLC-MS/MS conducted on a LTQ Orbitrap Velos mass spectrometer (Thermo Fisher Scientific). Representative of 2 independent experiments with similar results were obtained.

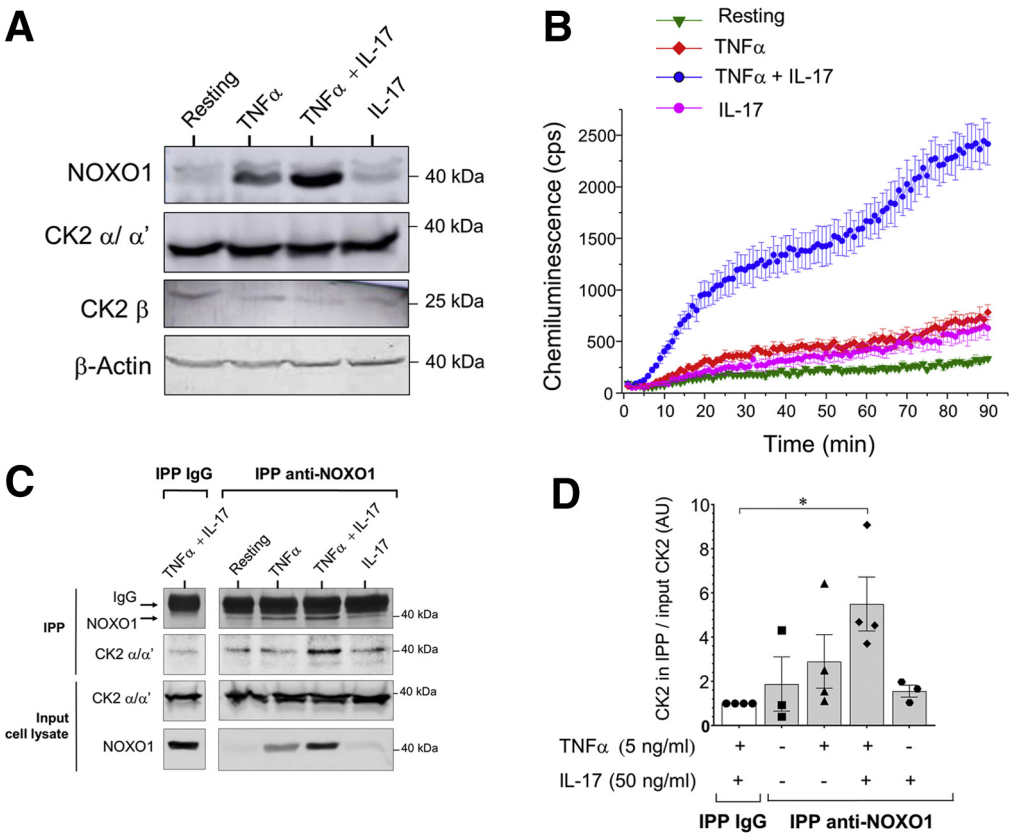


Figure 1. CK2 interacts with NOXO1 in T84 colon epithelial cells under inflammatory conditions. (*A*) Immunoblots of NOXO1, CK2α/α', CK2β, and β-actin in colon T84 cells stimulated with TNFα (5 ng/mL) or IL17 (50 ng/mL) individually or in combination for 24 hours at 37°C. Representative of 3 independent experiments. (*B*) ROS production was measured by chemiluminescence in T84 cells stimulated as in (*A*). n = 3. (*C*) Immunoblots of CK2 α/α' in NOXO1 IPP from T84 cells stimulated as in (*A*). Representative of 4 independent experiments. (*D*) Densitometry analysis of CK2 α/α' in NOXO1 IPP as in (*C*), normalized to CK2 α/α'expression in cell lysates; n = 4; mean ± SEM; one-way ANOVA with Tukey multiple comparisons test; *$P < .05$. (*E*) Confocal microcopy of T84 cells co-stimulated or not with TNFα + IL17 for 24 hours at 37°C. NOXO1 (*green*), CK2 α/α' (*red*), DAPI (*blue*). Scale bar: 10 μm. Representative of 6 independent experiments.

TNFα + IL17 (Figure 1*C* and *D*). Confocal microscopy showed co-localization of NOXO1 and CK2α/α' at the plasma membrane and in the nucleus of TNFα + IL17-stimulated cells (Figure 1*E*).

To determine whether CK2 interacts directly and specifically with NOXO1, dot-blot experiments were next performed as described in Methods, using recombinant NOXO1, $p47^{PHOX}$ (organizer subunit of phagocyte NOX2), NOXA1, or $p67^{PHOX}$ (activator subunit of NOX2) (Figure 2*A*). Interestingly, CK2 interacted with NOXO1 and $p47^{PHOX}$ but not with NOXA1 and $p67^{PHOX}$ (Figure 2*B*). Bovine serum albumin (BSA), the negative control, did not interact with CK2. To identify the region of NOXO1 involved in CK2 interaction, GST fusion proteins of the NOXO1 full-length (β isoform), N-terminal (1-157), and C-terminal regions (232-371) were constructed (Figure 2*C*) to perform pull-down experiments of CK2 from T84 epithelial cells lysates. CK2 α/α' was pulled down by the NOXO1 full-length and N-terminus but not by the NOXO1 C-terminus (Figure 2*D* and *E*). These experiments identified CK2 as a major NOXO1 partner in colon T84 epithelial cells and revealed a direct interaction that is mediated by the N-terminal region of NOXO1 that mostly contains the Phox homology (PX) domain.

CK2 Phosphorylates Recombinant NOXO1 on Several Sites

The direct interaction of CK2 with NOXO1 suggested that NOXO1 could be phosphorylated by CK2. We therefore

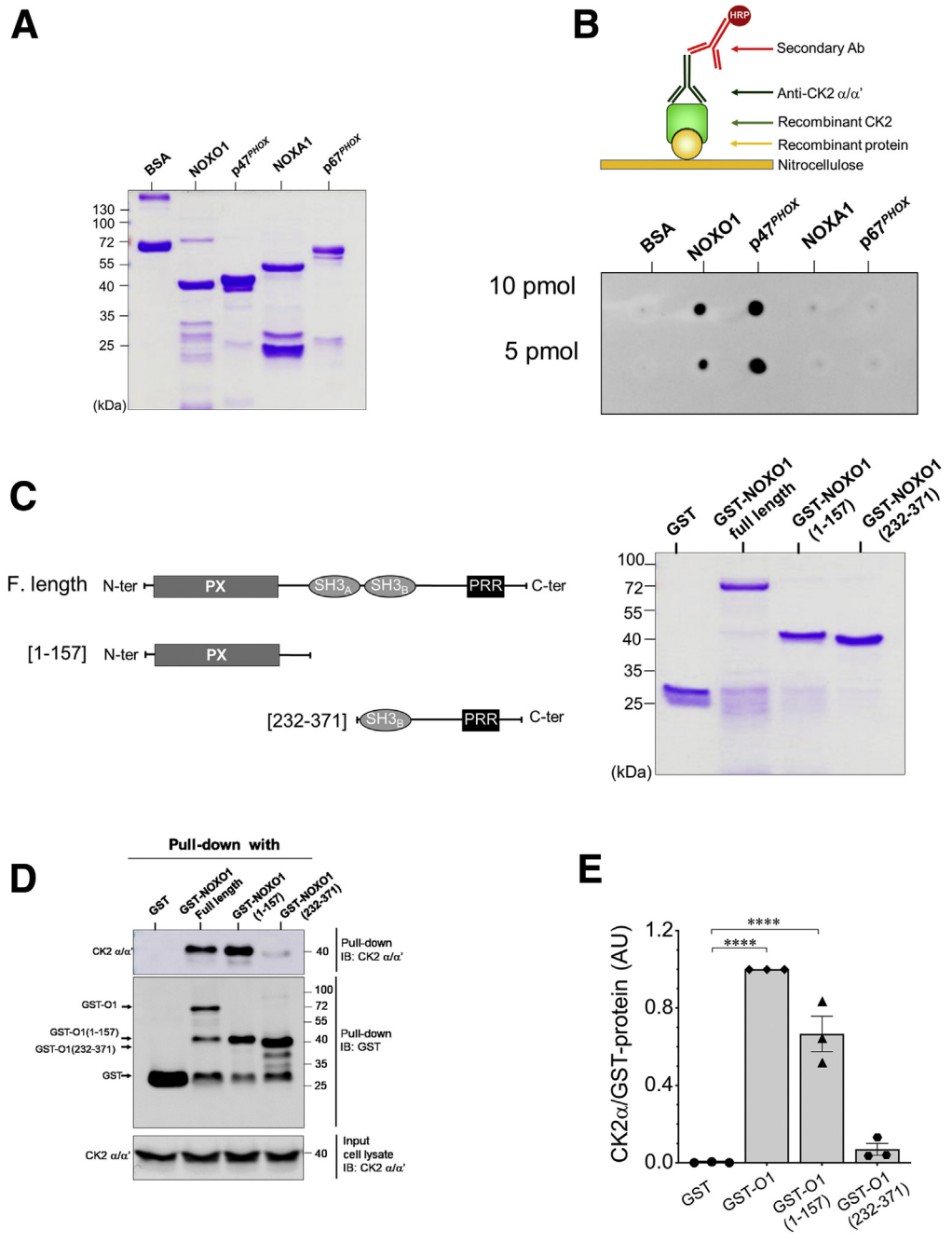


Figure 2. CK2 interacts directly with NOXO1 through the N-terminal region mostly containing the PX domain. (*A*) Coomassie Blue staining of recombinant NOXO1, $p47^{PHOX}$, NOXA1, and $p67^{PHOX}$. (*B*) Dot-blot analysis of interaction between CK2 and recombinant NOXO1, $p47^{PHOX}$, NOXA1, or $p67^{PHOX}$. Representative of 3 independent experiments. (*C*) Schematic representation and Coomassie Blue staining of GST fusion proteins of the NOXO1 full-length (β isoform), N-terminal (1-157), and C-terminal regions (232-371). (*D*) Pull-down of CK2 from resting T84 cells lysates by full-length GST-NOXO1, GST-NOXO1 (1-157), GST-NOXO1 (232-371), or GST (control). Representative of 3 independent experiments. (*E*) Densitometry analysis of CK2 α/α' pull-downed as in (*D*), normalized to GST-fusion proteins; n = 3; mean ± SEM; one-way ANOVA with Tukey multiple comparisons test; $^{****}P < 0.0001$.

analyzed phosphorylation of recombinant NOXO1 by constitutively active CK2 *in vitro*.

First, incorporation of ^{32}P into NOXO1 was monitored and analyzed by autoradiography. CK2 phosphorylated NOXO1 within minutes (Figure 3*A*, left), and no ^{32}P incorporation was detected in the absence of CK2 (Figure 3*A*, right). The phosphorylated sites on NOXO1 were next identified by nanoscale liquid chromatography coupled to tandem mass spectrometry (nanoLC-MS/MS). Seventy-six percent of the recombinant protein was covered by MS/MS, and several phosphorylated peptides were detected (Figure 3*B*). The position of the phosphorylated sites was estimated by A-score and highlighted in red in the sequence (Figure 3*B*). The C-terminus of NOXO1 was heavily phosphorylated by CK2 as shown by the identification by MS/MS of several phosphopeptides covering this region (Figure 3*B*). The extracted-ion chromatogram (XIC) showed 3 distinct elution peaks for 3 distinct phosphorylation sites corresponding to Ser-368, Thr-373, and Thr-374, the numbering referring to the γ isoform sequence (Figure 3*C*). A representative MS/MS spectrum of the phosphorylated C-terminus peptide at position 368 is shown in Figure 3*D*. These

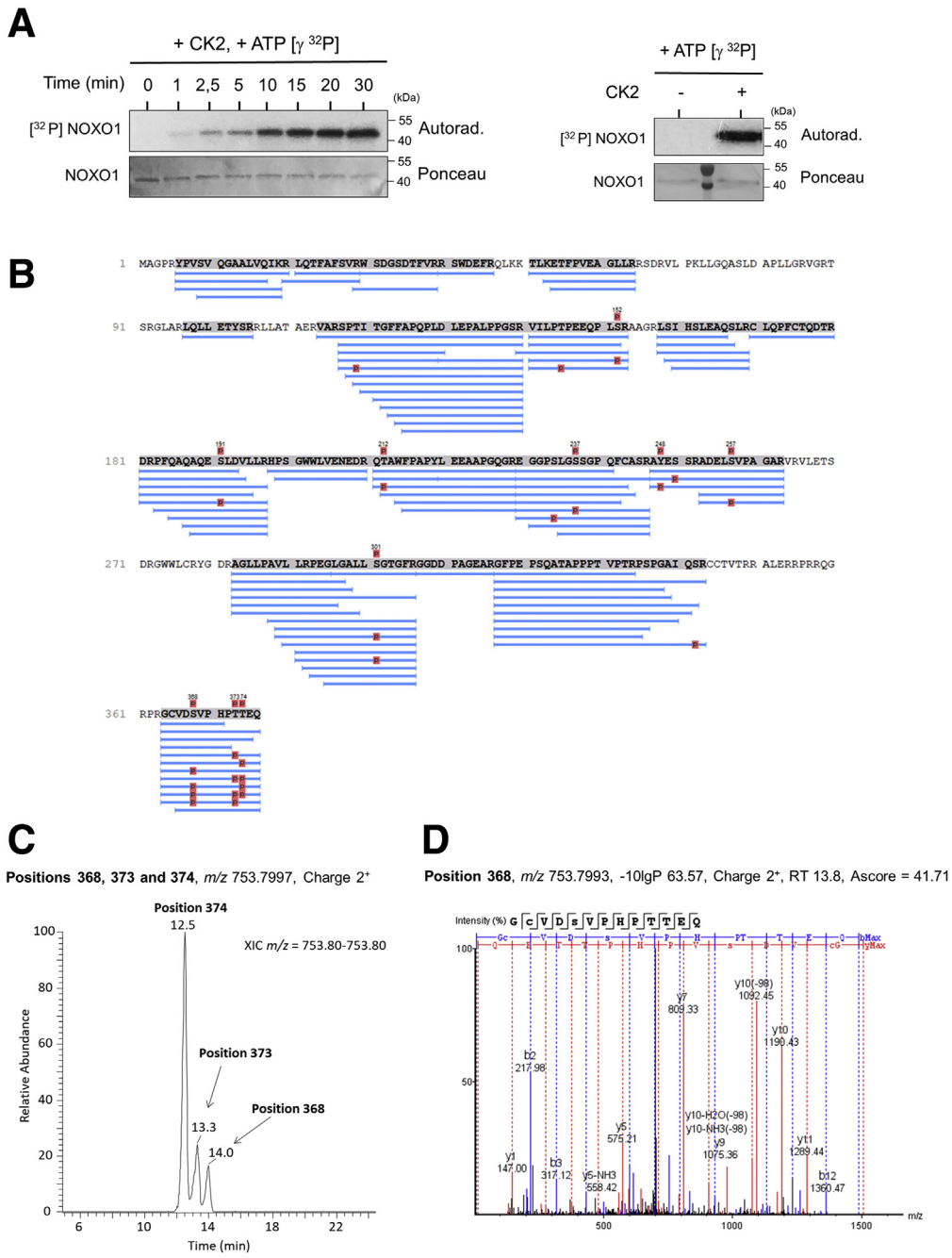


Figure 3. CK2 phosphorylates recombinant NOXO1 *in vitro* on several sites. (*A*) Autoradiography of recombinant NOXO1 phosphorylated with constitutively active CK2 in the presence of radioactive [γ^{-32P}] ATP. Time course (*left*), with or without CK2 (*right*). Representative of 3 independent experiments. (*B*) MS/MS protein coverage of recombinant NOXO1 after *in vitro* phosphorylation by CK2. Peptides were filtered according to 1% false discovery rate that corresponds to an identification score value >37.6 (–10lgP) with the software Peaks Studio Xpro. The confidence of modification sites is estimated by an Ascore, which calculates an ambiguity score as $-10 \times \log_{10}(p)$. The *P* value indicates the likelihood that the peptide is matched by chance (Ascore = 20 for *P* value of .01). Only confident modification sites with Ascore >20 were retained and their position labeled (*red*). (*C*) XIC of the heavily C-terminus phosphorylated peptide of *m/z* 753.997 showing 3 distinct elution peaks for 3 distinct phosphorylation sites. (*D*) Representative MS/MS spectrum of the phosphorylated C-terminus peptide at position 368. The confidence of modification sites is estimated by an Ascore (Ascore = 20 for *P* value of .01).

data show that NOXO1 is a good substrate for CK2 and that the phosphorylated sites may be located within the C-terminus.

Inhibition of CK2 Enhances ROS Production by NOX1 in Colon Epithelial Cells and Colonoids Under Inflammatory Conditions

To determine the functional relationship between CK2 and NOX1, we analyzed the effect of selective inhibitors of CK2 on NOX1 activity in T84 colonic epithelial cells and colonoids. First, CX-4549, a small molecule acting as a potent ATP competitor with a highly selective profile for CK2,[22] was tested in T84 cells. CX-4549 at 1 μmol/L increased ROS production by NOX1 in cells co-stimulated by TNFα + IL17, whereas it had no effect on resting cells (Figure 4*A*), which have low NOXO1 expression as shown in Figure 1*A*. Under similar conditions, CX-4549 also inhibited CK2 activity, as shown by the decrease in the phosphorylation profile of CK2 substrates detected with the phospho-CK2-substrate antibody (Figure 4*B*). CX-4549 did not impact NOXO1 expression (Figure 4*B*). The effect of CX-4549 on ROS production was concentration-dependent and occurred at concentrations below 2 μmol/L (Figure 4*C*), which did

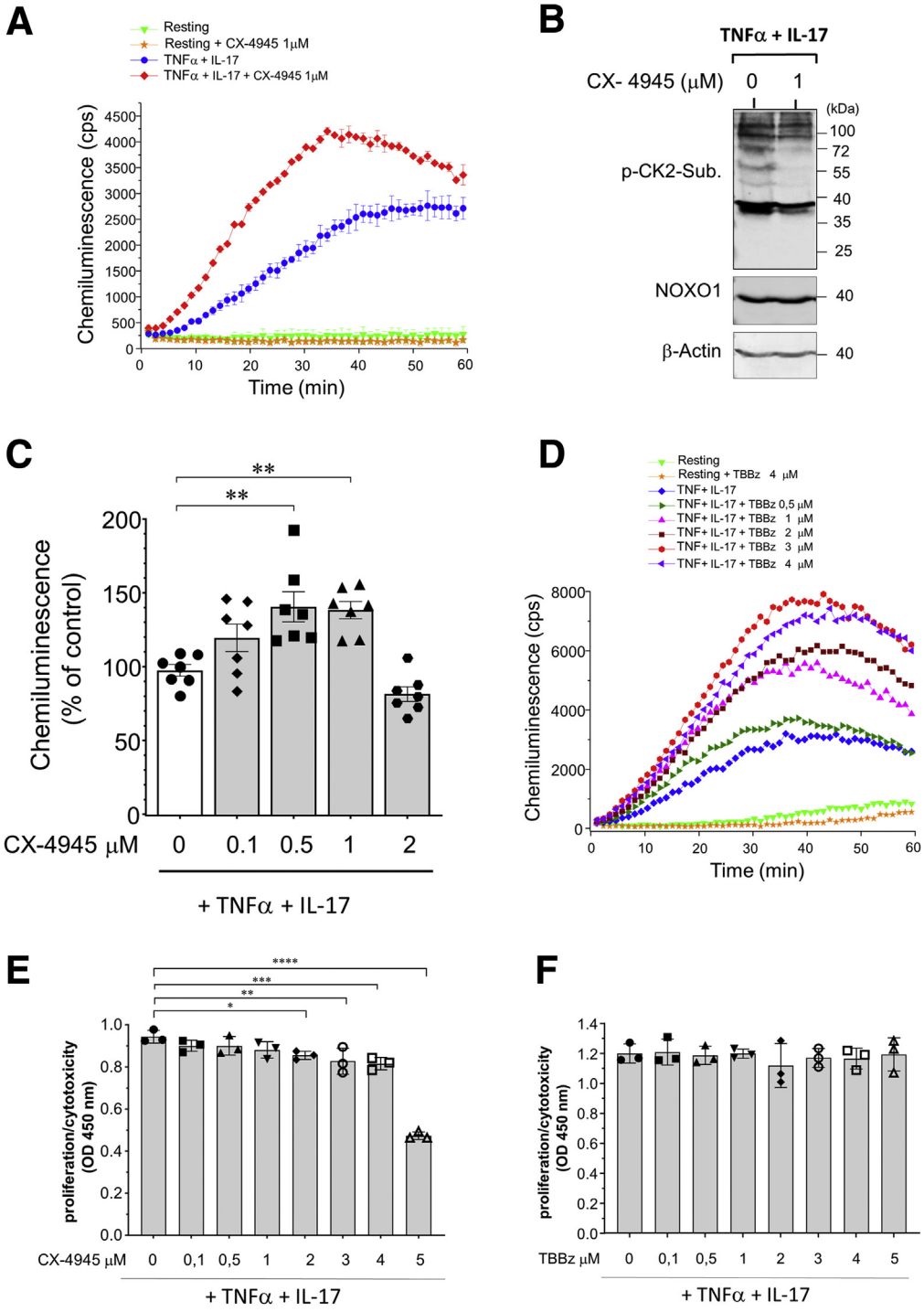


Figure 4. Inhibition of CK2 enhances ROS production by NOX1 in colon T84 epithelial cells under inflammatory conditions. (*A*) ROS production was measured by chemiluminescence in T84 cells co-stimulated or not with TNFα + IL17 in presence or absence of 1 μmol/L CX-4945 after 24-hour incubation at 37°C. n = 3. (*B*) CK2 activity *(top)* assessed with the phospho-CK2-substrate [(pS/pT)DXE] antibody and NOXO1 expression *(middle)* in T84 cells co-stimulated as in *(A)*. Representative of 3 independent experiments. (*C*) Concentration-dependent effect of CX-4549 on ROS production by NOX1 in T84 cells co-stimulated as in *(A)* in presence or absence of various concentrations of CX-4945 for 24 hours at 37°C. Data were expressed as percentage of control (cells treated with TNFα + IL17 in absence of CX-4549); n = 7 per condition; mean ± SEM; one-way ANOVA with Tukey multiple comparisons test; $^{**}P < .01$. **(***D***)** Concentration-dependent effect of TBBz on ROS production by NOX1 measured by chemiluminescence in T84 cells co-stimulated as in *(A)* in the presence or absence of various concentrations of TBBz for 24 hours at 37°C. **(***E***)** Concentration-dependent effect of CX4945 on proliferation/cytotoxicity of T84 epithelial cells. n = 3 per condition; mean ± SEM; one-way ANOVA with Dunnett multiple comparisons test; $^{*}P < .05$, $^{**}P < .01$, $^{***}P < .001$, $^{****}P < .0001$. **(***F***)** Concentration-dependent effect of TBBz on proliferation/cytotoxicity of T84 epithelial cells. n = 3 per condition; mean ± SEM.

not affect proliferation or cell toxicity (Figure 4*E*). Above 2 μmol/L CX-4549, some antiproliferative and cytotoxic effect could be observed, indirectly impacting ROS production (Figure 4*C* and *E*). To ascertain that inhibition of CK2 led to an increase of ROS production by NOX1, tetrabromobenzimidazole (TBBz), another selective CK2 inhibitor,[23] was used. TBBz enhanced the ROS production of T84 epithelial cells co-stimulated by TNFα + IL17 in a concentration-dependent manner (Figure 4*D*). TBBz did not show antiproliferative or cytotoxic effect at the concentrations used (Figure 4*F*). Thus, inhibition of CK2 results in an enhancement of NOX1 activity in colon T84 epithelial cells.

Next, the effect of CX-4945 on ROS production was analyzed in human colon organoids derived from biopsies of patients undergoing routine colonoscopy.[8] As in T84 epithelial cells, the combination of TNFα + IL17 strongly increased NOXO1 expression in colon organoids but had no effect on CK2α/α' and CK2β expression; the latter was also very weakly expressed in primary cells (Figure 5*A*). Increased NOXO1 expression induced by TNFα + IL17 was also associated with an increase in ROS production by colon organoids as compared with non-stimulated ones (Figure 5*C* and *D*). Treatment with 1 μmol/L CX-4945 did not affect the growth of colon organoids (Figure 5*B*) but significantly augmented ROS production in colon organoids co-stimulated with TNFα + IL17 as compared with those untreated by CX-4945 (Figure 5*C* and *D*). We also assessed ROS production in organoids by nitroblue tetrazolium (NBT) reduction and analyzed the resulting formazan deposits by phase contrast microscopy as described in Methods. Figure 5*E* shows a representative image of NBT reduction in organoids. Far more intense formazan deposits could be observed in colon organoids co-stimulated with TNFα + IL17 as compared with unstimulated organoids. Treatment with 1 μmol/L CX-4945 further increased formazan deposits in colon organoids co-stimulated with TNF α + IL17, and some deposits could also be observed in unstimulated ones (Figure 5*E*). Together, these data show that CK2 inhibition resulted in enhancement of ROS production by NOX1, indicating that CK2 negatively regulates NOX1 activity in T84 colon epithelial cells and in colon organoids under inflammatory conditions.

CK2 Activity Is Decreased During Acute Colitis Induced by the Hapten Reagent TNBS

Because NOX1 and CK2 are emerging as important regulators of immunity and inflammation in the intestines, we next examined their expression and activity during acute colitis induced by TNBS in mice. We have previously shown that TNBS-induced colitis was dependent on NOX1 activity because NOX1-deficient mice were protected against disease progression.[8] This model is characterized with secretion of various potent proinflammatory cytokines, including TNFα and IL17, and establishment of a transmural inflammation that resembles the histopathologic lesions found in human CD.[24] In mice treated with TNBS, the colon weight/length ratio and Wallace score, reflecting colon macroscopic damage and severity,[25] were both increased (Figure 6*A*). Histologic examination of the colon showed extensive ulceration and abundant infiltration of inflammatory cells accompanied by crypt loss (Figure 6*B*). Strikingly, CK2 activity was significantly reduced during acute colitis induced by TNBS, as revealed by the decrease in phosphorylation profile of CK2 substrates detected with the phospho-CK2-substrate antibody in the cytosolic and membrane fractions of colon homogenates (Figure 6*C* and *D*). Moreover, expression of the CK2 α/α' subunits in the colon did not change during acute colitis, whereas expression of the CK2β subunit significantly increased, indicating that the drop in CK2 activity was not due to a decrease in expression of its subunits (Figure 6*E* and *F*). Concurrently to the decrease in CK2 activity, a strong augmentation of the expression of the NOX1 and $p22^{PHOX}$ subunits forming the membrane catalytic core of the NOX1 complex was observed in mouse colons during TNBS-induced acute colitis (Figure 6*G* and *H*). In addition, NOXO1 mRNA was also increased, whereas NOXA1 mRNA did not change (Figure 6*I*).

Because CK2 appears to undergo an intra-steric regulation that involves an autoinhibition of its α catalytic subunit by the β regulatory subunit,[26] we hypothesized that increased expression of the CK2β subunit during TNBS-induced colitis could be responsible for the decrease in CK2 activity through its autoinhibitory action on CK2α/α'. To test this hypothesis, we overexpressed Myc-CK2β or CK2α in T84 colonic epithelial cells (Figure 7*A*) and analyzed the impact on CK2 activity and ROS generation. Overexpression of Myc-CK2β regulatory subunit decreased CK2 activity, whereas overexpression of the CK2α catalytic subunit increased CK2 activity, as evidenced by the analysis of the phosphorylation profile of CK2 substrates (Figure 7*B*). This strongly supports that increased expression of the CK2β subunit can down-regulate CK2 activity in epithelial cells. Furthermore, under stimulation with IL17 + TNFα overexpression of the β regulatory subunit, which resulted in decreased CK2 activity, enhanced ROS production in colonic epithelial cells (Figure 7*C*, left), whereas overexpression of the α catalytic subunit, which resulted in increased CK2 activity, reduced it (Figure 7*C*, right). This confirms the role of CK2 activity in limiting ROS generation. In addition, phosphorylation of NOXO1 by CK2 *in vitro* was decreased in the presence of increasing concentrations of recombinant CK2β (rec. CK2β) (Figure 7*D*). Interestingly, the recombinant β regulatory subunit was itself a very good substrate for CK2 (Figure 7*D*). Together, these data suggest that increased expression of the CK2β subunit during TNBS-induced colitis may down-regulate CK2 activity and consequently phosphorylation of NOXO1 by CK2, thereby lifting the blocking effect of CK2 on the generation of ROS by NOX1.

The Highly Selective CK2 Inhibitor, CX-4945, Exacerbates TNBS-Induced Colitis

Because we showed that CK2 can limit ROS production by NOX1 in colon epithelial cells and that CK2 activity is decreased during TNBS-induced colitis, we hypothesized that the drop in CK2 activity could contribute to the increase

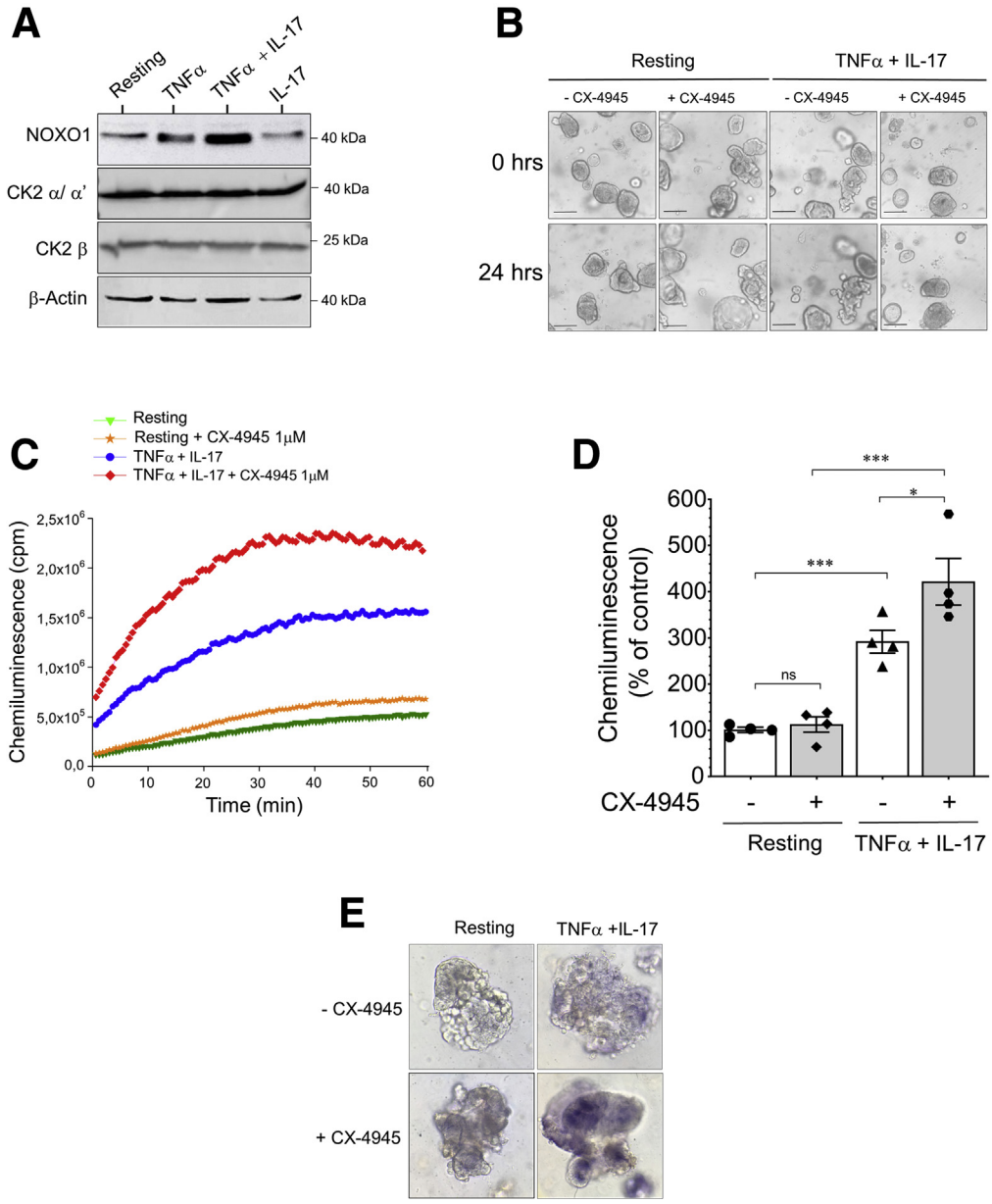
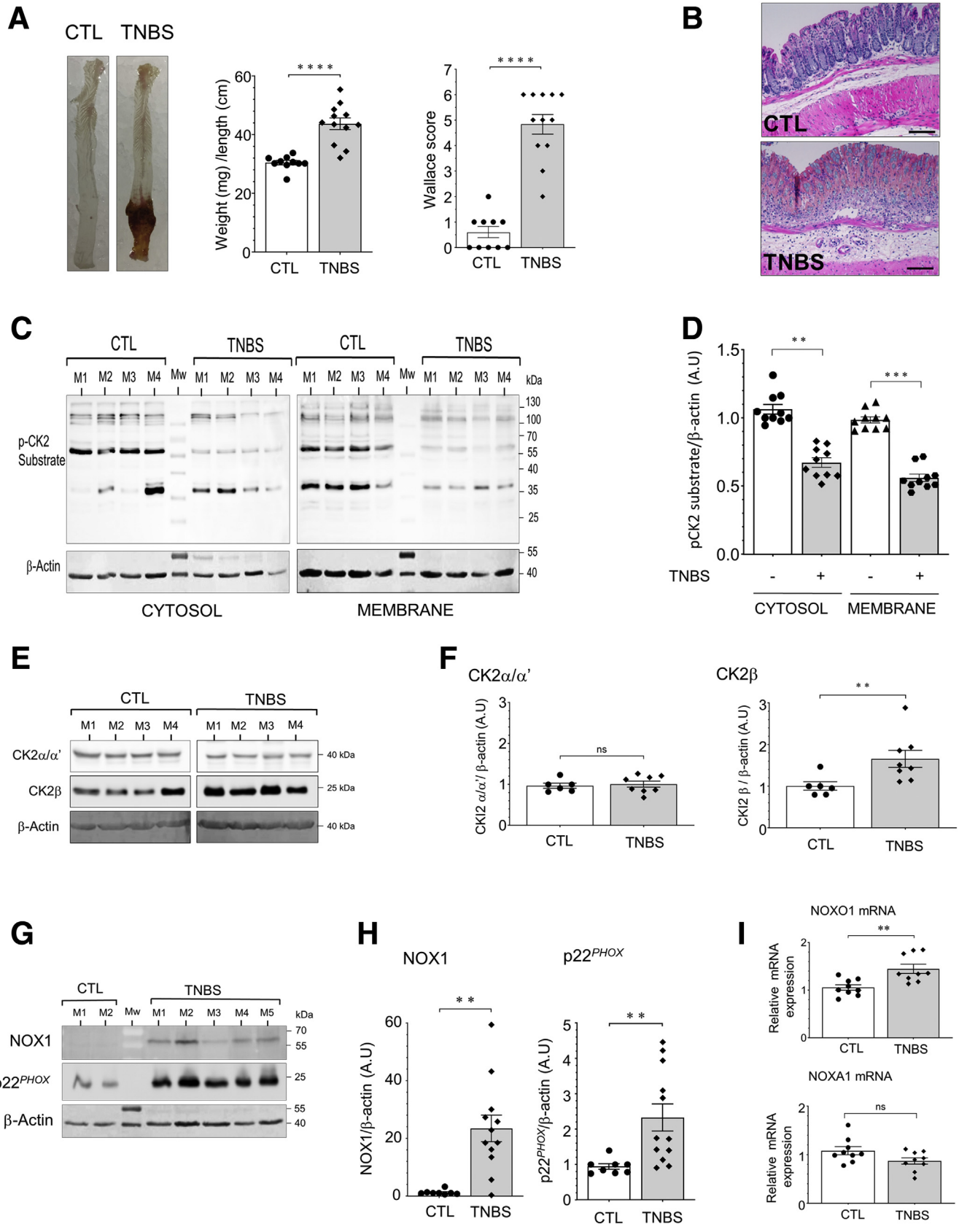


Figure 5. Inhibition of CK2 enhances ROS production by NOX1 in colon organoids under inflammatory conditions. (*A*) Representative immunoblots of NOXO1, CK2α/α', CK2β, and β-actin in colon organoids stimulated as in Figure 1*A* for 24 hours at 37°C. (*B*) Representative images of colon organoids established from colon biopsies of control patients. At day 8, organoids were co-stimulated or not with TNFα + IL17 in presence or absence of 1 μmol/L CX-4945 for 24 hours at 37°C. Scale bar: 100 μm. (*C*) ROS production was measured by chemiluminescence in colon organoids treated as in *(B)*. (*D*) Data as in *(C)* were quantified and expressed as percentage of control (resting cells in the absence of CX-4549); n = 4 per condition; mean ± SEM; one-way ANOVA with Tukey multiple comparisons test; **P* < .05, ****P* < .001. (*E*) ROS production by organoids treated as in *(B)* was assessed by NBT reduction. Phase contrast microcopy with ×400 magnification.

in ROS production during TNBS-induced colitis, thereby promoting oxidative stress and colon damage. To the best of our knowledge, there are no known inducers of CK2 activity that can be used to determine whether restoration of CK2 activity could provide protection. Therefore, we determined whether further inhibition of CK2 by CX-4945 could exacerbate inflammation and oxidative stress during TNBS-induced colitis. Mice received intraperitoneal injection of CX-4945 (25 mg/kg) or dimethyl sulfoxide (DMSO) (for control groups) twice at 2 hours before and 6 hours after TNBS challenge. At the macroscopic level, CX-4945 increased the area of colon damage (Figure 8*A*), and histologic evaluation of the colons revealed more severe damage of the colon in the TNBS group treated with CX-4945 (Figure 8*B* and *C*). Thus, the intestinal architecture in the TNBS group treated with CX-4945 was profoundly impacted, with extensive necrosis and complete erosion of epithelial crypts and presence of congested vessels, accompanied by a marked transmural infiltration of inflammatory cells (Figure 8*B*). The intestinal architecture was less severely affected in the group receiving only TNBS, because inflammatory cells within the mucosa and submucosa were still present but did not invade the transmural area (Figure 8*B*). Worsening of histologic damage in the presence of CX-4945 was reflected by an increase of the Ameho score[27] (Figure 8*C*). In addition, this was associated with increased levels of markers of inflammation, such as CXCL1, in the TNBS-mice treated with CX-4945 as compared with those in the TNBS control group (Figure 8*D*). ROS production was assessed *ex vivo* in colon tissue sections using NBT reduction. Colons, processed as described in Methods, were incubated for 1 hour at 37°C with NBT, and


A
CTL TNBS
Weight (mg) /length (cm)
****
CTL TNBS
Wallace score
****
CTL TNBS
B
CTL
TNBS
C
CTL TNBS CTL TNBS
M1 M2 M3 M4 Mw M1 M2 M3 M4 M1 M2 M3 M4 Mw M1 M2 M3 M4
kDa
130
100
70
55
40
35
25
55
40
p-CK2 Substrate
β-Actin
CYTOSOL MEMBRANE
D
pCK2 substrate/β-actin (A.U)
**
***
TNBS - + - +
CYTOSOL MEMBRANE
E
CTL TNBS
M1 M2 M3 M4 M1 M2 M3 M4
CK2α/α'
CK2β
β-Actin
40 kDa
25 kDa
40 kDa
F
CK2α/α'
CKI2 α/α'/ β-actin (A.U)
ns
CTL TNBS
CK2β
CKI2 β / β-actin (A.U)
**
CTL TNBS
G
CTL TNBS
M1 M2 Mw M1 M2 M3 M4 M5
kDa
NOX1
p22PHOX
β-Actin
70
55
25
55
40
H
NOX1
NOX1/β-actin (A.U)
**
CTL TNBS
p22PHOX
p22PHOX/β-actin (A.U)
**
CTL TNBS
I
NOXO1 mRNA
Relative mRNA expression
**
CTL TNBS
NOXA1 mRNA
Relative mRNA expression
ns
CTL TNBS

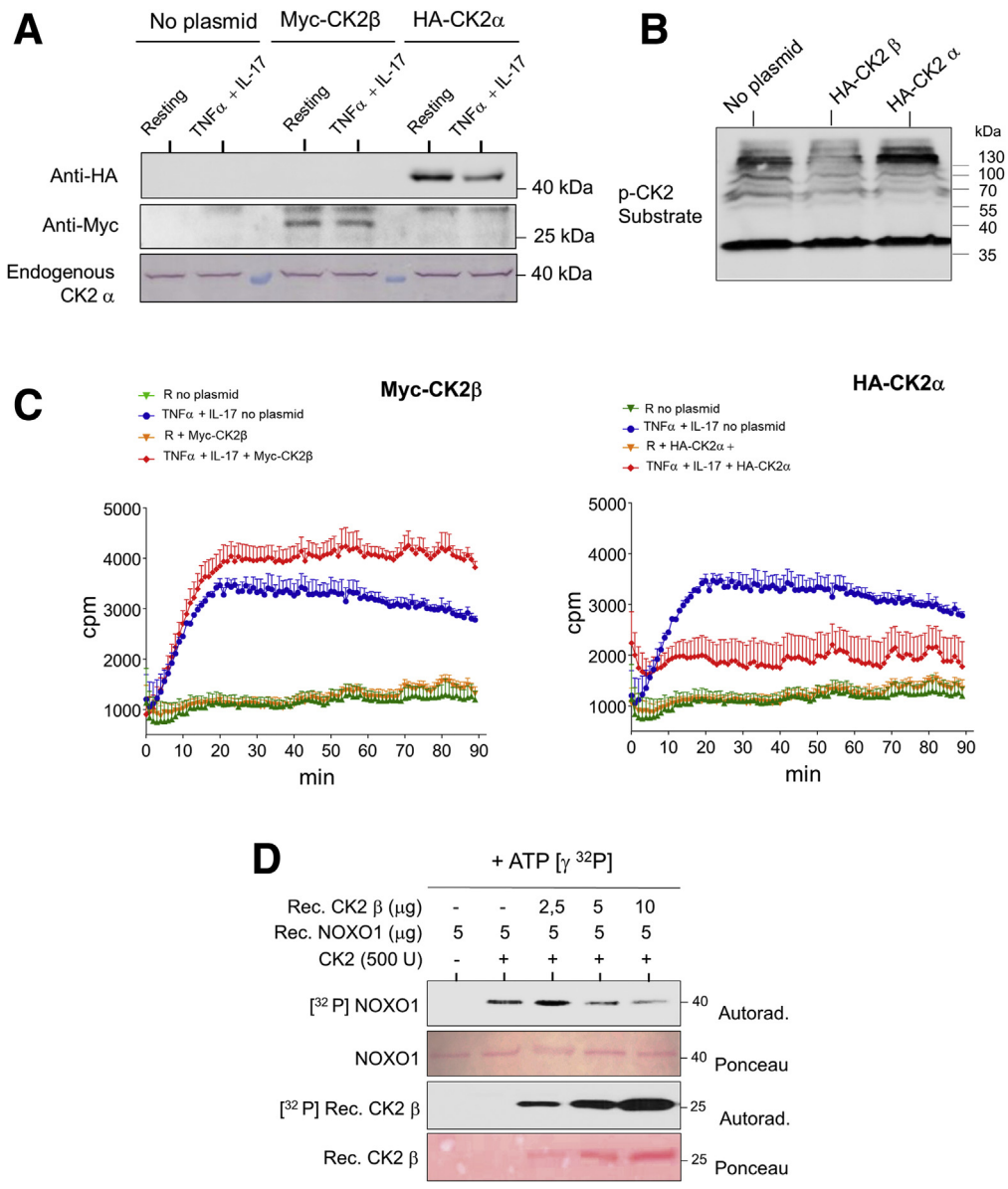


Figure 7. Effect of CK2β and CK2α overexpression on CK2 activity and ROS production in colon T84 epithelial cells. (*A*) Immunoblots of HA-CK2β and Myc-CK2α overexpressed individually in colon T84 cells. (*B*) CK2 activity assessed with the phospho-CK2-substrate [(pS/pT)DXE] antibody in T84 cells overexpressing CK2β or CK2α. (*C*) ROS production was measured by chemiluminescence in T84 cells overexpressing CK2β or CK2α. n = 3. (*D*) Effect of increasing concentrations of recombinant CK2β subunit on phosphorylation of NOXO1 by CK2 *in vitro*. Autoradiography (Autorad.) and Ponceau-Red are shown.

Figure 6. (***See previous page***). **CK2 activity is highly reduced and NOX1 expression is increased during TNBS-induced acute colitis.** (*A*) *Left,* representative image of colons 24 hours after injection of TNBS or vehicle (CTL); *middle,* weight/length ratio changes after TNBS treatment; *right,* macroscopic lesions as assessed by Wallace score. Mean ± SEM, ≥10 animals; Mann-Whitney test; ****$P < .0001$. (*B*) Histologic images of colons 24 hours after TNBS-induced colitis (original magnification, ×200) as compared with CTL (vehicle). Scale bar: 50 μm. (*C*) CK2 activity in cytosolic and membrane fractions of colon homogenates assessed 24 hours after injection of TNBS or vehicle (CTL) with the phospho-CK2-substrate antibody. Four mice are shown (M1 to M4) for each group. (*D*) Densitometry analysis of p-CK2 substrates normalized to β-actin expression. Mean ± SEM from 10 animals; Kruskal-Wallis test with Dunn multiple comparisons test; **$P < .01$, ***$P < .001$. (*E*) Immunoblots of CK2α/α' and CK2β in colon homogenates 24 hours after injection of TNBS or vehicle (CTL). Four mice are shown (M1 to M4) for each group. (*F*) Densitometry analysis of CK2α/α' and CK2β normalized to β-actin expression. Mean ± SEM, ≥6 animals; Mann-Whitney test; **$P < .01$. (*G*) Immunoblots of NOX1 and p22^{PHOX} in colon homogenates 24 hours after injection of TNBS or vehicle (CTL). Two mice (M1 to M2) in the CTL group and 5 mice (M1 to M5) in the TNBS group are shown. (*H*) Densitometry analysis of NOX1 and p22^{PHOX} normalized to β-actin expression. Mean ± SEM, ≥8 animals; Mann-Whitney test; **$P < .01$. (*I*) Expression of NOXO1 and NOXA1 RNA messengers during TNBS-induced acute colitis. Relative expression levels for each gene were calculated using the $2^{-\Delta\Delta Ct}$ method, with normalization to the average and GAPDH housekeeping genes. Mean ± SEM, 9 animals; Mann-Whitney test; **$P < .01$.

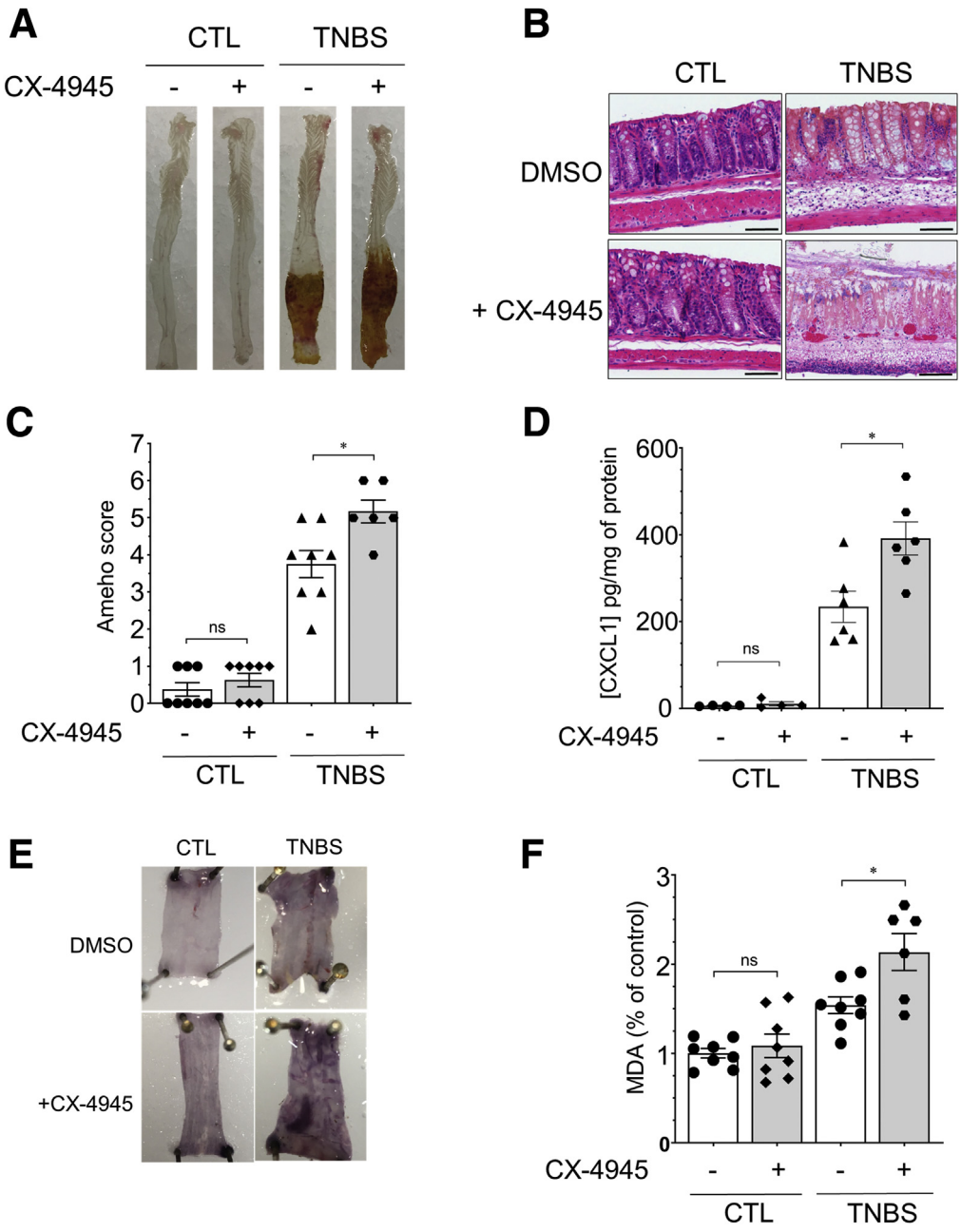


Figure 8. The highly selective CK2 inhibitor CX-4945 exacerbates TNBS-induced colitis. (*A*) Representative images of colons 24 hours after injection of TNBS or vehicle (CTL) in mice treated with the CK2 inhibitor CX-4945 (25 mg/kg) or DMSO. (*B*) Histologic images of colons 24 hours after TNBS-induced colitis (original magnification, ×200) as compared with CTL (vehicle) in mice treated with the CK2 inhibitor CX-4945 (25 mg/kg) or DMSO. Scale bar: 50 μm. (*C*) Histologic damage of colon as assessed by the Ameho score in mice treated as in *(B)*. Mean ± SEM, ≥6 animals; Mann-Whitney test; **P* < .05. (*D*) Secretion of CXCL1 (pg. mg^{-1} protein) in colons of mice treated as in *(B)*. Mean ± SEM from 4 animals (CTL groups with and without CX-4945) to 6 animals (TNBS groups with and without CX-4945), Mann-Whitney test; **P* < .05. (*E*) ROS production assessed *ex vivo* by NBT reduction in colon tissue of mice treated as in *(B)*. Formazan deposits were examined macroscopically. Representative of 4 mice in the CTL groups with and without CX-4945 and at least 7 mice in the TNBS groups with and without CX-4945. (*F*) MDA (nmol. mg^{-1} protein) content in the colon of mice treated as in *(B)*, normalized as compared with control. Mean ± SEM, ≥6 animals; Mann-Whitney test; **P* < .05.

reduction of NBT was examined macroscopically. Formazan deposits were increased in colons from TNBS-treated mice as compared with control mice, and the presence of CX-4945 intensified NBT reduction, indicating higher ROS production (Figure 8*E*). To confirm that CX-4945 contributed to *in vivo* ROS-mediated colon damage, malondialdehyde (MDA), a product of lipid peroxidation induced by oxidative stress, was measured in colon homogenates. A significant increase in MDA content in colons of TNBS-treated mice was observed in the presence of CX-4945 as

compared with those treated only with TNBS (Figure 8*F*). Altogether, the above data show that CK2 activity was strikingly decreased, whereas expression of NOX1 was upregulated in mice during TNBS-induced acute colitis. Moreover, decreasing CK2 activity even further with CX-4945 exacerbated TNBS-induced colitis concomitantly with increased CXCL1 levels, ROS production, and lipid peroxidation.

In contrast to the TNBS-induced colitis, it has been shown in previous studies that inhibition of CK2 by CX-4945 had no effect in dextran sulfate sodium (DSS)-induced colitis[21]; thus, we aimed to understand the reasons for these divergent observations. In addition to the dependence of TNBS-induced colitis on NOX1 activity,[8] the present study suggests that CX-4945 exacerbates TNBS-induced colitis by promoting excessive activation of NOX1 in epithelial cells. Therefore, we sought to determine whether DSS-induced colitis showed any dependence on NOX1 activity. For this purpose, we used NOX1-deficient mice to induce DSS colitis. A 2.5% w/v DSS was administered in NOX1$^{y/-}$ and wild-type (WT) mice for 7 consecutive days. NOX1-deficient mice were not protected against DSS-induced colitis as compared with WT mice (Figure 9). Mice exhibited body weight loss, increased fecal occult blood score, colon shortening, and macroscopic lesions reflected by the Wallace score comparable to WT mice (Figure 9*A*–*C*). They also exhibited crypt lesions and mucosal inflammatory cell infiltration similar to WT mice (Figure 9*D*). Furthermore, in the DSS model, no increase of NOX1 could be observed at the protein and mRNA levels in WT mice (Figure 9*E* and *F*), contrary to the observations in the TNBS model. In addition, NOXO1 and NOXA1 mRNAs did not change during DSS-induced colitis in WT and NOX$^{y/-}$ mice (Figure 9*F*). Regarding p22^{PHOX}, only a slight increase could be observed at the mRNA level during DSS-induced inflammation (Figure 9*F*). Together, these data indicate that in contrast to the TNBS model, DSS-induced colitis is not dependent on NOX1, which might explain the absence of effect of CX-4945 in the DSS model.

Discussion

NOX1 has emerged as a crucial regulator of intestinal mucosa immunity and homeostasis through its ability to coordinate several important epithelial cell functions.[3] Because ROS are highly toxic molecules, mechanisms modulating their production at the right place and right level must exist. In the case of NOX1, which has been shown in many studies to be constitutively active,[28] the question arises of how the flow of ROS produced by NOX1 is controlled to allow beneficial effects while avoiding oxidative damage, a driving factor of IBD.

In the present study, we show that CK2 is a major partner of NOXO1 and directly binds and phosphorylates NOXO1. Consequently, CK2 decreased NOX1 activity and ROS production in colon epithelial cells. Furthermore, our data suggest that in TNBS-induced colitis, a model where disease progression is dependent on NOX1 activity,[8,29] a drop in CK2 activity combined with increased NOX1 expression may result in excessive ROS production, thereby contributing to the progression of inflammation and colon damage.

Our study reveals that CK2 specifically and constitutively binds to NOXO1 and that this binding occurs after induction of NOXO1 expression by TNFα + IL17. CK2 binds to the N-terminus (1-157) of NOXO1, which mainly encompasses the PX domain (1-131), a structural motif known to be involved in phosphoinositide binding.[30] Although our experimental conditions do not allow to conclude that the PX domain is responsible for CK2 binding, it is interesting to put forth such speculation, because PX domains are known to bind to cytoskeleton proteins such as moesin,[31] and many cytoskeleton-associated functions are regulated by CK2.[32]

Our data show that CK2 phosphorylates NOXO1 on several sites *in vitro*. In particular, the C-terminus was heavily phosphorylated on Ser-368, Thr-373, and Thr-374. Surprisingly, most of the sites phosphorylated by CK2 on NOXO1 (Figure 3*B*) do not fit the classical CK2 consensus site, characterized by the presence of an acidic residue at position n+3. Interestingly, non-canonical CK2 consensus sites have been shown to be targeted by CK2 on the human p53 protein, and in addition, although being classified as a protein serine/threonine kinase, CK2 is also able to catalyze phosphorylation on tyrosine in mammalian cells.[33,34]

Although our data clearly show that NOXO1 phosphorylation by CK2 limits NOX1 activity, the underlying mechanisms remain to be determined. One possibility is that phosphorylation of NOXO1 by CK2 may favor the intramolecular interaction between the bis-SH3 and the proline-rich region domains, thus impeding optimal binding of NOXO1 to p22^{PHOX} and NOX1 activity.[35,36] On the other hand, phosphorylation of NOXO1 by CK2 may modulate phosphorylation on other sites, especially those involved in the activation of the NOX1 complex such as Ser-159 (equivalent of Ser-154 on β isoform).[15] Indeed, we and others have shown that the NOXO1 β isoform can be phosphorylated by PKC on Ser-154 in transfected cell systems such as HEK293 and CHO cells and that this phosphorylation enhanced NOX1 activity.[15,16] In epithelial cells, NOXO1 could probably be phosphorylated by CK2 and by PKC, which has been shown to play a crucial role in the development of different types of colitis.[37] One could postulate that phosphorylation of NOXO1 by CK2 might restrict NOX1 activity, whereas phosphorylation by PKC would enhance NOX1 activity. Therefore, a decrease of CK2 activity associated with an increase of PKC activity during intestinal inflammation may promote excessive ROS production by NOX1, thereby contributing to oxidative stress damage. Further studies are needed to support this hypothesis.

The restrictive function of CK2 regarding NADPH oxidase activity is not unique to NOX1. Indeed, it has been shown that CK2 binds to p47^{PHOX}[38] and phosphorylates it *in vitro*.[39] In addition, it was found that DRB, the first identified CK2 inhibitor, potentiated fMLF-induced NOX2 activity in DMSO-differentiated HL60 cells.[39] In accordance, we found that CK2 also binds to recombinant p47^{PHOX}, the NOX2 organizer subunit, but not to p67^{PHOX} or to NOXA1 (Figure 2*B*). Regarding DUOX2, which is also expressed in intestinal

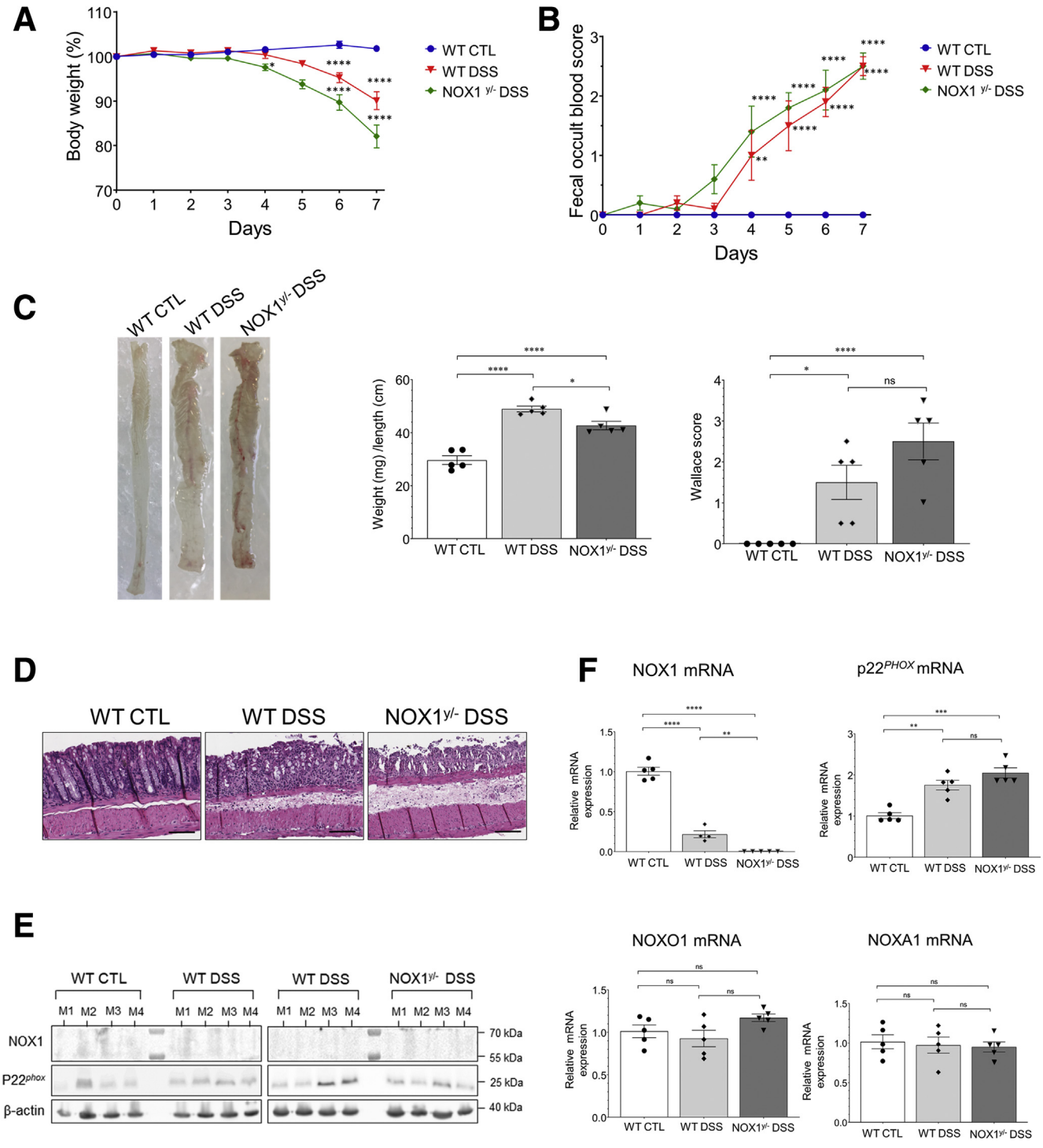


Figure 9. NOX1 is not involved in DSS-induced colitis. (*A*) Body weight loss of WT and NOX1-deficient (NOX1$^{y/-}$) mice during DSS-induced colitis. WT CTL, wild-type mice control; WT DSS, wild-type mice treated with DSS; *NOX1*$^{y/-}$ DSS, NOX1-deficient mice treated with DSS. Mean ± SEM from 5 animals; two-way ANOVA Tukey multiple comparisons test; *$P < .05$, ****$P < .0001$ as compared with WT CTL. (*B*) Fecal occult blood score of WT and NOX1-deficient (NOX1$^{y/-}$) mice during DSS-induced colitis. Mean ± SEM from 5 animals; two-way ANOVA Tukey multiple comparisons test; **$P < .01$, ****$P < .0001$ as compared with WT CTL. (*C*) *Left,* representative image of colons from WT and NOX1$^{y/-}$ mice at day 7 after DSS treatment; *middle,* weight/length ratio changes after DSS treatment; *right,* macroscopic lesions as assessed by Wallace score. Mean ± SEM from 5 animals; Mann-Whitney test; *$P < .05$, ****$P < .0001$. (*D*) Histologic images of colons from WT and NOX1$^{y/-}$ mice at day 7 after DSS-induced colitis (original magnification, ×200) as compared with WT CTL (vehicle). Scale bar: 50 μm. (*E*) Immunoblots of NOX1 and p22^{PHOX} in colon homogenates of WT and NOX1$^{y/-}$ mice at day 7 after DSS-induced colitis as compared with CTL (vehicle). Four mice in each group (M1 to M4). (*F*) NOX1, NOXO1, NOXA1, and p22^{PHOX} mRNA levels were assessed in colons of WT and NOX1$^{y/-}$ mice at day 7 after DSS-induced colitis as compared with WT CTL (vehicle). Relative expression levels for each gene were calculated using the $2^{-\Delta\Delta Ct}$ method, with normalization to the average and GAPDH housekeeping genes. Mean ± SEM, 5 animals; Mann-Whitney test; **$P < .01$, ***$P < .001$.

epithelial cells, it does not appear to be regulated by CK2. Indeed, the CK2 inhibitor CX-4945 did not impact the activity of DUOX2 transfected in HEK-293 cells (Figure 10), which is consistent with the fact that CK2 tends to primarily target NOX isoforms that use an organizing subunit.

The present study also showed that CK2 activity is highly reduced during TNBS-induced acute colitis, a phenomenon that was also observed during DSS-induced acute colitis.[19] Being a constitutive kinase, one would expect the decrease in CK2 activity to correlate with a decrease in expression. Indeed, the decrease in CK2 activity in DSS-induced acute colitis was associated with a clear diminution of expression of the CK2α/α' subunits.[19] In contrast, the level of CK2α/α' subunits did not change significantly in TNBS-induced acute colitis, and the level of the CK2β subunit was actually increased. Our data suggest that increased expression of the CK2β subunit may be responsible for the decrease in CK2 activity. Indeed, overexpression of the β regulatory subunit in colon epithelial cells decreased phosphorylation of CK2 substrates. Interestingly, we found that the β regulatory subunit is a very good substrate for CK2, in accordance with previous studies.[40] Therefore, the β regulatory subunit of CK2 may compete with NOXO1 to decrease its phosphorylation by CK2. Decreased CK2 activity resulting from the CK2β regulatory subunit overexpression was associated with increased ROS generation; in contrast, increased CK2 activity resulting from CK2α catalytic subunit overexpression was associated with decreased ROS generation. This confirms that CK2 limits ROS production.

We also found that the drop in CK2 activity in TNBS-induced acute colitis occurred concomitantly with an increase in the expression of the NOX1 subunits and in ROS production and MDA levels. The link between the decrease in CK2 activity and the increase in NOX1 subunit expression during TNBS-induced colitis is not clear, because the highly selective CK2 inhibitor CX-4945 did not further increase NOX1 subunit expression in mice colons (Figure 11). However, decreasing CK2 activity with CX-4945 potentiated both ROS production and MDA levels concomitantly with the exacerbation of inflammation and colon damage.

Recently, it has been shown that CK2 inhibition with CX-4945 limits immune-mediated colitis progression, predominantly through *in vivo* inactivation of claudin-2 pores.[21] The authors also showed no apparent *in vivo* toxicities from CX-4945 in the DSS model. However, our study shows that CX-4945 exacerbated inflammation in the TNBS-induced colitis model. Contrary to the TNBS model, we found that DSS-induced colitis was not dependent on NOX1, which might explain the absence of effect of CX-4945 in the DSS model (Figure 9). In addition, Koch et al[19] demonstrated that CK2 is a critical regulator of epithelial homeostasis during chronic intestinal inflammation. Therefore, we cannot rule out that exacerbation of TNBS-induced colitis by CX-4945 could be also related to defect in intestinal epithelial cell restitution that is controlled by CK2 via β-catenin signaling.[19]

In summary, our study reveals a new role for the widely expressed, constitutively active protein kinase, CK2, as a molecular brake of NOX1 activity in colonic epithelial cells and a potential mechanism for the excessive ROS production during intestinal inflammation. This study also opens a new avenue for treating inflammatory diseases of the intestines such as IBD, because strategies to activate CK2 could be a

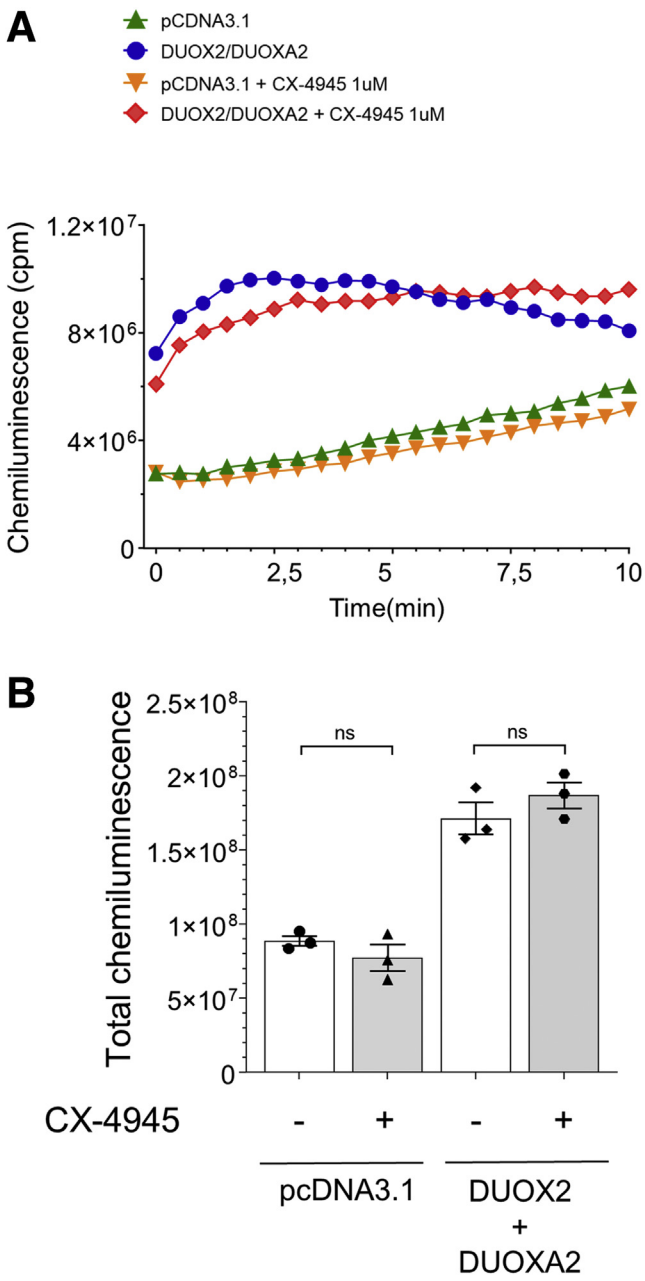


Figure 10. Effect of CX-4945 on DUOX2 activity. (*A*) DUOX2 and DUOXA2 in pCDNA3.1 were transfected in HEK-293 cells in serum-free medium using the FuGENE HD reagent. Cells were dissociated using a non-enzymatic solution, suspended in Hank's balanced salt solution, and counted. ROS production was measured by luminol-amplified chemiluminescence after activation of DUOX2 with 1 μmol/L ionomycin and PMA (500 ng/mL) in the presence of HRPO. Light emission was expressed in counted photons per minute (cpm). (*B*) Total chemiluminescence in each experimental condition expressed as mean ± SEM of 3 independent experiments.

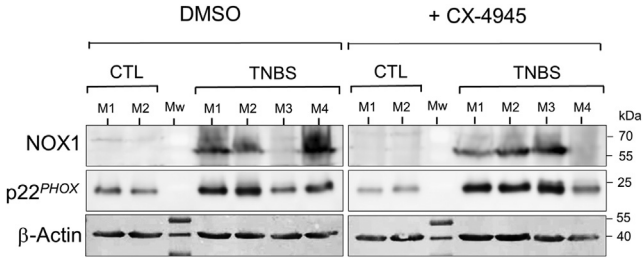


Figure 11. Expression of NOX1 and p22^{PHOX} during TNBS-induced acute colitis in the presence or absence of CX-4945. Immunoblots of NOX1 and p22^{PHOX} in colon homogenates 24 hours after injection of TNBS or vehicle (CTL) in mice treated with the CK2 inhibitor CX-4945 (25 mg/kg) or DMSO. Results from 2 mice (M1 to M2) in the CTL group and 4 mice (M1 to M4) in the TNBS group are shown.

novel therapeutic approach. Finally, the study highlights that some caution should be exercised when using the highly selective CK2 inhibitor CX-4945 that exacerbated intestinal inflammation, warranting further toxicity studies, especially as it is now tested in a Phase II clinical trial.

Methods

Antibodies and Reagents

CK2α and CK2β plasmids were from Addgene (Teddington, UK). Antibodies directed against human NOXO1 and NOXA1 were produced as previously described.[14,15] Anti-human NOX1 was from Genetex (Irvine, CA), and the anti-mouse NOX1 was produced by Genecust (Ellange, Luxembourg) using an internal immunogen sequence of NOX1. Anti-ph22^{PHOX} and anti-GST were from Santa Cruz Biotechnology (Heidelberg, Germany). Antibodies directed against CK2 α/α' and β were from Santa Cruz Biotechnology. Phospho-CK2 Substrate [(pS/pT)DXE] antibodies were purchased from Cell Signaling Technology (Danvers, MA). Anti-β-actin was from Sigma-Aldrich (Saint-Quentin Fallavier, France). Secondary horseradish peroxidase–labelled goat anti-rabbit or anti-mouse antibodies and secondary alkaline phosphatase-labelled goat anti-rabbit or anti-mouse antibodies were from Santa Cruz Biotechnology. TNF-α and IL17 were from PeproTech France (Neuilly-Sur-Seine, France).

Mice

WT male C57BL/6J mice (Janvier Laboratories, Le Genest-St-Isle, France) or Nox1$^{Y/-}$-deficient mice (The Jackson Laboratory, Sacramento, CA) were bred under specific pathogen-free conditions and used at 10–12 weeks of age.

Cell and Colon Organoid Cultures

T84 colon epithelial cells from ATCC-LGC (Molsheim, France) were cultured as described in our previous work.[8] Biopsies obtained after approval by the Bichat Hospital Institutional Review Board from patients without IBD undergoing routine colonoscopy were used to establish colon organoids that were cultured in Corning Matrigel Matrix as described in our previous work.[8]

Cell Transfection

T84 colon epithelial cells were seeded to reach 80% confluence. They were then transfected in serum-free medium using the T84 Cell Avalanche Transfection Reagent (EZ Biosystems, College Park, MD), prepared in complexes with plasmid DNA according to the manufacturer's instructions (15 μL of T84 Cell Avalanche Transfection Reagent for 5 μg of total DNA: pRC/CMV, pRC/CMV HA-CK2α, and/or pRC/CMV Myc-CK2β). Serum-free medium was replaced by serum-containing medium 5 hours after transfection, and the cells were cultured for 48 hours before use.

Induction of Colitis in Mice

In TNBS model, after overnight food deprivation, acute colitis was induced in mice by intrarectal administration under ketamine/xylazine anesthesia of TNBS (40 μL, 150 mg/kg), dissolved in 1:1 mixture of 0.9% NaCl with 100% ethanol. Control mice received only the 1:1 mixture of 0.9% NaCl with 100% ethanol. Animals were killed 24 hours after TNBS administration. In DSS model, colitis was induced in NOX1$^{y/-}$ and WT mice by administering 2.5% w/v DSS, Reagent grade (MP Biomedicals, Illkirch, France), dissolved in drinking water for 7 days as described by Chassaing et al.[41] Mice were killed on day 7. Body weight, stool consistency, and presence of occult blood in feces (0–4) were assessed daily.

Treatment With Cytokines and CK2 Inhibitors

Cells and colon organoids were treated with TNFα (5 ng/mL) and IL17 (50 ng/mL) either individually or in combination for 24 hours at 37°C. In some assays, two CK2 inhibitors, CX-4945 (Selleckchem, Souffelweyersheim, France) and TBBz (Merck, Darmstadt, Germany), were added at the indicated concentrations just before cytokine treatment. In the TNBS experiments, mice were injected twice intraperitoneally with CX-4945 (25 mg/kg) or DMSO (for control group) 2 hours before and 6 hours after the TNBS challenge.

Cytotoxicity Assay

The effect of increasing concentrations of CX4945 or TBBz on proliferation/cytotoxicity of T84 cells was assessed using the Cyto-X Cell Proliferation/Cytotoxicity Kit (Cell Applications Inc, San Diego, CA) according to the manufacturer's instructions and as previously described.[8]

Co-immunoprecipitation Experiments

For co-immunoprecipitation studies of CK2 α/α' with NOXO1, T84 cells were stimulated with cytokines or buffer and lysed in lysis buffer containing 20 mmol/L Tris-HCl (pH 7.6), 0.5% TX-100, 100 mmol/L NaCl, 2.5 mmol/L EGTA, 2.5 mmol/L EDTA, 10 μg/mL leupeptin, 10 μg/mL pepstatin, 10 μg/ml aprotinin, 1 mmol/L PMSF, 1 mg/mL NaF, 0.5 mg/ml β-glycerophosphate, 0.5 mg/mL PNPP, 0.2 mg/mL levamisole, 1 mmol/L DTT, and 8% D(+)-Saccharose. Resting and

stimulated cell lysates were incubated with rabbit polyclonal NOXO1 antibody or rabbit IgG control antibody for 2 hours at 4°C, and then immobilized protein A agarose was added, and the assay was incubated for an additional 2 hours. Co-immunoprecipitated CK2 α/α' was detected with a mouse monoclonal anti-CK2 α/α' antibody.

In Vitro Phosphorylation Assay

Recombinant NOXOβ was phosphorylated with constitutively active CK2 (New England Biolabs, Evry, France) by incubating 10 μg (or 5 μg where indicated) of protein in a reaction mixture containing 40 mmol/L HEPES (pH 7.5), 10 mmol/L $MgCl_2$, 10 mmol/L dithiothreitol (DTT), 100 μmol/L ATP, and 3 μCi of [γ^{-32P}] ATP (Hartmann Analytic GmbH, Braunschweig, Germany) in a total volume of 50 μL at 30°C for 30 minutes or for different times from 0 to 30 minutes. In some assays recombinant human CK2β protein (GeneTex Inc, Irvine, CA) was added. The reaction was stopped by adding hot 5× Laemmli sample buffer. Proteins were separated by sodium dodecyl sulfate-polyacrylamide gel electrophoresis (SDS-PAGE), transferred to nitrocellulose, and revealed by autoradiography. Authorization to use radioactivity was obtained under no. ASN T751061.

LC-MS/MS Analyses

For identification of NOXO1 partners, T84 cells were stimulated with a combination of TNFα and IL17 and lysed in lysis buffer as described above. Cell lysates were incubated with rabbit polyclonal NOXO1 antibody or rabbit IgG control antibody for 2 hours at 4°C, and immobilized protein A agarose was then added and incubated for an additional 2 hours. IPP were washed 4 times with lysis buffer and subjected to SDS-PAGE for low migration (5 mm). The gels were stained with Coomassie Blue. A 50/50 mixture of ACN/NH_4HCO_3 50 mmol/L was used to destain gel plugs. Proteins were then in gel-digested overnight with sequencing grade trypsin (Promega, Madison, WI) at 37°C in a 25 mmol/L NH_4HCO_3 buffer (0.2 μg trypsin in 20 μL). The resulting peptides were desalted using ZipTip μ-C18 Pipette Tips (Pierce Biotechnology; Rockford, IL) according to the manufacturer's instructions. Peptide mixtures were analyzed by a Q-Exactive Plus coupled to a Nano-LC Proxeon 1000, both from Thermo Fisher Scientific (Waltham, MA). Peptides were separated by chromatography using Acclaim PepMap100 C18 pre-column (0.075 × 20 mm, 3 μm, 100 Å), Pepmap-RSLC Proxeon C18 column (0.075 × 500 mm, 2 μm, 100 Å), 300 nL/min flow rate, and a 98-min gradient from 95% solvent A (H_2O/0.1% FA) to 35% solvent B (100% ACN/0.1% FA), followed by column regeneration for a total time of 120 minutes. Peptides were analyzed in the Orbitrap cell in positive mode at a resolution of 70,000, with a mass range of *m/z* 200-2000 and an AGC target of 3.10^6. MS/MS data were acquired in the Orbitrap cell in a Top20 mode. Raw data were processed on a Proteome Discoverer 2.1 with the mascot node (Mascot version 2.5.1; Matrix Sciences, Mount Prospect, IL). MS/MS spectra were searched against the Swissprot protein database release 2016_05 with the *Homo Sapiens* taxonomy and a maximum of 2 missed cleavages. Precursor and fragment mass tolerances were set to 6 ppm and 0.02 Da, respectively. Identified proteins obtained with the rabbit polyclonal NOXO1 antibody versus rabbit IgG control antibody were qualitatively compared using mascot scores, the number of identified peptides, and coverage parameters between each condition to determine potential protein partners of NOXO1. The experiment was performed sequentially in 2 periods of time with 3 replicates in total to confirm repeatability.

For the *in vitro* identification of phosphorylation sites, triplicate samples of recombinant NOXO1 phosphorylated *in vitro* by CK2 (New England Biolabs Inc) versus controls were digested to their liquid form by adding 20 μL of 25 mmol/L NH_4HCO_3 buffer containing 0.2 μg of sequencing-grade trypsin and incubating overnight at 37°C. The resulting peptides were loaded and desalted on Evotips provided by Evosep (Odense, Denmark) according to the manufacturer's procedure. Samples were analyzed on an Orbitrap Fusion mass spectrometer (Thermo Fisher Scientific) coupled with an Evosep one system (Evosep) operating with the 30SPD method developed by the manufacturer. Briefly, the method is based on a 44-minute gradient and a total cycle time of 48 minutes with a C18 analytical column (0.15 × 150 mm, 1.9 μm beads, ref EV-1106) equilibrated at room temperature and operated at a flow rate of 500 nL/min. H_20/0.1% FA was used as solvent A and ACN/0.1% FA as solvent B. The mass spectrometer was operated in data-dependent acquisition. Peptide masses were analyzed in the Orbitrap cell in full ion scan mode at a resolution of 120,000, a mass range of m/z 350-1550, and an AGC target of 4.10^5. MS/MS was performed in the top speed 3s mode. Peptides were selected for fragmentation by Higher-energy C-trap Dissociation with a normalized collisional energy of 27% and a dynamic exclusion of 60 seconds. Fragment masses were measured in an Ion trap in the rapid mode, with an AGC target of 1.10^4. Monocharged peptides and unassigned charge states were excluded from the MS/MS acquisition. The maximum ion accumulation times were set to 100 msec for MS and 35 ms for MS/MS acquisition. Raw data were processed on the PEAKS X+ Studio software (Bioinformatics Solutions Inc, Waterloo, ON, Canada). De Novo was run with the following parameters: trypsin as enzyme, half of a disulfide bridge (C) as fixed, and deamidation (NQ)/oxidation (M) as variable modifications. Precursor and fragment mass tolerance were set to 15 ppm and 0.5 Da, respectively. Database search was conducted against the Swissprot protein database release 2020_06 with the *Homo Sapiens* taxonomy and a maximum of 2 missed cleavages. Phosphorylation (STY) as a variable modification was added to previous De Novo parameters to identify phosphorylation sites. The maximum variable PTM per peptide was set to 4. Spectra were filtered using a 1% false discovery rate. The confidence of modification sites is estimated by an Ascore, which calculates an ambiguity score as $-10 \times \log10(p)$. The *P* value indicates the likelihood that the peptide is matched by chance (Ascore = 20 for a *P* value of .01).

Expression and Purification of Recombinant Proteins

NOXO1β, NOXO1β (1-157), NOXO1β (232-371), p47^{PHOX}, NOXA1, and p67^{PHOX} were subcloned in pGEX-6P1 vector (GE Healthcare, Chicago, IL) and were expressed in *Escherichia coli* (BL21) as GST fusion proteins and purified with glutathione Sepharose beads as described previously.[14,15]

Dot-blots

Ten or five picomoles of recombinant NOXO1β, p47^{PHOX}, NOXA1, p67^{PHOX}, and BSA (Sigma-Aldrich, Lyon, France) were applied directly on nitrocellulose membrane in a single spot and let to air dry. The membranes were blocked for 1 hour at room temperature in TBS/T (20 mmol/L Tris-HCl [pH 7.6], 137 mmol/L NaCl, 0.1% Tween 20) containing 5% nonfat dry milk and then incubated with 1 μg/mL recombinant CK2 (New England Biolabs) diluted in TBS/T containing 1% fat dry milk overnight at 4°C. After several washes with TBS/T, bound CK2 was detected with a mouse monoclonal anti-CK2 α/α' antibody at 1/1000 dilution for 1 hour at room temperature. Antibody binding was detected using horseradish peroxidase–conjugated anti-mouse IgG. Blots were visualized using ECL Western blotting reagents.

GST Pull-Down Assay

Recombinant GST-NOXO1β, GST-NOXO1β (1-157), or GST-NOXO1β (232-371) at 286 nmol/L were incubated with T84 cell lysates for 30 minutes at 4°C on a rotating wheel. Glutathione Sepharose beads were then added, and incubation was continued for an additional 1 hour at 4°C. After washing, complexes were eluted with 10 mmol/L glutathione and analyzed by SDS-PAGE and Western blot using protein-specific antibodies.

Confocal Microscopy

T84 cells were detached, fixed in suspension with 4% paraformaldehyde for 10 minutes, and permeabilized with 0.5% TX-100 in phosphate-buffered saline (PBS) for 10 minutes at room temperature. The autofluorescence of residual paraformaldehyde was quenched by incubating the cells in 50 mmol/L NH4Cl for 5 minutes. After washing and resuspending in PBS, the cell suspension was spin-coated on slides with a Cytospin centrifuge and blocked with 5% BSA in PBS. Cells were then incubated for 1 hour at room temperature with a rabbit anti-NOXO1 polyclonal antibody (1:50) and a mouse anti-CK2α/α' antibody (1:400) diluted in 0.1% BSA in PBS. After washing, cells were incubated with an Alexa Fluor 488 (green)-conjugated goat anti-rabbit antibody (1:400) and Alexa Fluor 568 (red)-conjugated goat anti-mouse antibody (1:400) for 1 hour at room temperature in the dark. Nuclei were counterstained with DAPI Staining Solution (Thermo Fisher Scientific). Stained cells were examined with a Leica (Wetzlar, Germany) SP8-Tandem confocal microscope, a 488-nm argon laser, and 561-nm diode laser, and the images were imported into the Leica Application Suite X for analysis.

ROS Production

After treatment of T84 cells with TNFα (5 ng/mL) + IL17 (50 ng/mL) in the presence or absence of various concentrations of CX-4945 for 24 hours at 37°C, cells were washed and suspended in Hank's balance salt solution. ROS production by T84 cells was measured by luminol-amplified chemiluminescence in the presence of horseradish peroxidase in the Spark multimode microplate reader (Tecan, Mannedorf, Switzerland). Phorbol myristate acetate (PMA) (500 ng/mL) was added to optimize the detection of NOX1 activity[8]; light emission was expressed in counted photons per second (cps). Regarding colon organoids, after treatment with cytokines in the presence or absence of 1 μmol/L CX-4945 for 24 hours at 37°C, the culture three-dimensional Matrigel domes were washed and then broken up with gentle cell dissociation reagent (Stemcell Technologies, Grenoble, France), and organoids were trypsinized into single cells that were suspended in Hank's balanced salt solution and counted. ROS production was measured by luminol-amplified chemiluminescence in the presence of horseradish peroxidase in a Berthold (Oak Ridge, TN) 953 apparatus for 60 minutes at 37°C in the presence of PMA (500 ng/mL) for optimization of NOX1 activity detection. Light emission was expressed in counted photons per minute (cpm). ROS production by organoids was also assessed by NBT reduction and analyzed by phase contrast microscopy. Organoids, treated or not with TNFα (5 ng/mL) + IL17 (50 ng/mL) in the presence or absence of CX-4945 (1 μmol/L) for 24 hours at 37°C, were washed, recovered in Hank's balanced salt solution, and incubated 30 minutes at 37°C with NBT at 2 mg/mL in the presence of 500 ng/mL PMA for optimal activation of the NOX1 complex.[8] They were then fixed with formalin at 0.6% for 2 minutes, washed in 1 mL PBS by centrifugation at 290*g* for 5 minutes at 4°C, and suspended in 40 μL of PBS. Formation of formazan was examined under phase contrast microcopy with $\times$400 magnification. NBT reduction was also assessed *ex vivo* in mouse colon tissue sections. Colons were opened longitudinally, fixed face up on paraffin petri dishes, and incubated for 1 hour at 37°C with NBT at 2 mg/mL in Hank's balanced salt solution in the presence of 500 ng/mL PMA. Formazan deposits were examined macroscopically.

Macroscopic and Histologic Assessment of Colitis

Colonic inflammation was evaluated by the weight to length ratio of each intestine (anus to cecum). The colons were opened, and macroscopic lesions were evaluated according to the Wallace criteria and scores, which rate macroscopic lesions (0–10) on the basis of features reflecting inflammation such as hyperemia, thickening of the bowel, and extent of ulceration.[25] For histologic analysis, colon specimens located 1 cm above the anus were excised and embedded into paraffin. Several 5-μm paraffin sections were prepared and stained with hemalum-eosin. Sections were scored according to the Ameho criteria.[27]

Protein Extraction and Western Blot Analysis

Mouse colon tissues were homogenized using a rotor-stator, whereas T84 cells were lysed in lysis buffer on ice as previously published.[8] Protein concentration was determined by the Bradford method. Samples were analyzed for protein expression with target-specific antibodies using standard SDS-PAGE and immunoblotting techniques. The protein bands were quantified using Image J (Wayne Rasband, National Institutes of Health, Bethesda, MD).

Real-Time Polymerase Chain Reaction Assays

Total RNA was isolated from mouse colon tissue homogenates with TRIzol (Ambion; Life Technologies, Carlsbad, CA) according to manufacturer's protocol. RNA concentrations were measured with the DeNovix DS 11 Series Microvolume Spectrophotometer (Wilmington, DE). After removing potential genomic DNA contaminants with RNase-free DNase I (Thermo Fisher Scientific), the first cDNA strand was synthesized from RNA template by using RevertAid First Strand cDNA Synthesis Kit (Thermo Fisher Scientific). Real-time polymerase chain reactions were performed using the Roche LightCycler 480 device and the Kapa Sybr Fast qPCR kit (CliniSciences, Nanterre, France) according to the manufacturer's protocol. Samples were run in duplicates, and the melting curves and peaks were controlled for each primer pair. Relative expression levels for each gene were calculated by using the $2^{-\Delta\Delta Ct}$ method, with normalization to the average and GAPDH housekeeping genes. The primer sequences were the following: GADPH forward: 5′-CGT AGA CAA AAT GGT GAA GGT-3′, reverse: 5′ GAC TCC ACG ACA TAC TCA GC-3′; NOXA1 forward: 5′-TCT GCG CTG TGC TTC TTC TCA GAT-3′, reverse: 5′-AGG AAA TCC ATG GGC TCC AGA TGT-3′; NOXO1 forward: 5′-CCA TGC TGT AGC CTT GGT GCA AAT-3′, reverse: 5′-AAA CCA GGC TAC CTG CTG ATC CTT-3′; NOX1 forward: 5′-GGC ACC TGC TCA TTT TGC AAC-3′, reverse: 5′-CAG ATC ATA TAT GCC ACC AGC-3′; $p22^{PHOX}$ forward: 5′TGG ACG TTT CAC ACA GTG GT-3′, reverse: 5-5′-TGG ACC CCT TTT TCC TCT TT-3′.

Measurement of CXCL1 (KC)

Mouse colons were homogenized using a rotor-stator in buffer containing 20 mmol/L Tris-HCl pH 7.5, 250 mmol/L saccharose, 10 mmol/L EGTA, 2 mmol/L EDTA, 10 μg/mL leupeptin, 10 μg/mL pepstatin, 10 μg/mL aprotinin, and 1 mmol/L PMSF. Homogenates were ultracentrifuged at 100,000*g* for 1 hour at 4°C in a Beckman Coulter Optima Max-XP ultracentrifuge (Brea, CA). KC level was measured in the post-centrifugation supernatant using a commercially available Mouse KC ELISA kit (RayBiotech, Peachtree Corners, GA) according to the manufacturer's instructions.

MDA Content

MDA content was used as an indicator of lipid peroxidation. The adducts generated by the reaction of MDA with thiobarbituric acid allows the indirect measurement of MDA content. Colon tissues were homogenized and centrifuged as described above. The same volume of supernatant and trichloroacetic acid solution at 20% (containing 0.8% butylated hydroxytoluene to prevent nonspecific chromophore formation during the assay procedure) was mixed to precipitate proteins. After centrifugation at 1000*g* for 10 minutes, the resulting supernatant was mixed with Tris-TBA (26 mmol/L Tris and 120 mmol/L thiobarbituric acid) and 0.6 mol/L HCl in a volume ratio of 5:4:1 and heated in a water bath at 80°C for 15 minutes. The absorbance of the supernatants was measured with a Cary UV-Vis Multicell Peltier spectrophotometer (Agilent Technologies, Les Ulis, France) at 532 nm. A standard curve was established by preparing standard solutions containing various concentrations of MDA (0.25, 0.5, 1, and 2 mmol/L) from a 10 mmol/L stock solution (Elabscience Biotechnology, Houston, TX). The standard solutions were processed as the samples. Concentration of MDA was established against the standard curve, and MDA content was expressed as $nmol.mg^{-1}$ protein and normalized as compared with the control.

Statistics

Data were presented as mean ± standard error of the mean (SEM). Unpaired two-tailed Mann-Whitney rank tests were used for 2 group comparisons. One-way analysis of variance (ANOVA) with Tukey multiple comparison post-test or Kruskal-Wallis with Dunn multiple comparisons post-test were used for comparison of more than 2 groups as appropriate. Data were analyzed with Prism 8.4.3 (Graphpad Software, San Diego, CA), and $P < .05$ was considered statistically significant.

Study Approval

Animal studies were performed in accordance with the European Community Guidelines. All protocols were approved by the Bichat Ethics Committee for Animal Research (APAFIS authorization number 11901). Human biopsies required to establish colon organoids were obtained after approval by the Bichat Hospital Institutional Review Board. Informed consent for the experimental use of the tissues was obtained during the patient hospitalization.

References

1. Garrett WS, Gordon JI, Glimcher LH. Homeostasis and inflammation in the intestine. Cell 2010;140:859–870.
2. Peterson LW, Artis D. Intestinal epithelial cells: regulators of barrier function and immune homeostasis. Nat Rev Immunol 2014;14:141–153.
3. Dang PM, Rolas L, El-Benna J. The dual role of reactive oxygen species-generating nicotinamide adenine dinucleotide phosphate oxidases in gastrointestinal inflammation and therapeutic perspectives. Antioxid Redox Signal 2020;33:354–373.
4. Segal AW, Jones OT. Novel cytochrome b system in phagocytic vacuoles of human granulocytes. Nature 1978;276:515–517.
5. El Hassani RA, Benfares N, Caillou B, Talbot M, Sabourin JC, Belotte V, Morand S, Gnidehou S, Agnandji D, Ohayon R, Kaniewski J, Noël-Hudson MS, Bidart JM, Schlumberger M, Virion A, Dupuy C. Dual

oxidase2 is expressed all along the digestive tract. Am J Physiol Gastrointest Liver Physiol 2005;288:G933–G942.
6. Suh YA, Arnold RS, Lassegue B, Shi J, Xu X, Sorescu D, Chung AB, Griendling KK, Lambeth JD. Cell transformation by the superoxide-generating oxidase Mox1. Nature 1999;401:79–82.
7. Corcionivoschi N, Alvarez LA, Sharp TH, Strengert M, Alemka A, Mantell J, Verkade P, Knaus UG, Bourke B. Mucosal reactive oxygen species decrease virulence by disrupting Campylobacter jejuni phosphotyrosine signaling. Cell Host Microbe 2012;12:47–59.
8. Makhezer N, Ben Khemis M, Liu D, Khichane Y, Marzaioli V, Tlili A, Mojallali M, Pintard C, Letteron P, Hurtado-Nedelec M, El-Benna J, Marie JC, Sannier A, Pelletier AL, Dang PM. NOX1-derived ROS drive the expression of Lipocalin-2 in colonic epithelial cells in inflammatory conditions. Mucosal Immunol 2019;12:117–131.
9. Kawahara T, Kuwano Y, Teshima-Kondo S, Takeya R, Sumimoto H, Kishi K, Tsunawaki S, Hirayama T, Rokutan K. Role of nicotinamide adenine dinucleotide phosphate oxidase 1 in oxidative burst response to Toll-like receptor 5 signaling in large intestinal epithelial cells. J Immunol 2004;172:3051–3058.
10. Jones RM, Neish AS. Redox signaling mediated by the gut microbiota. Free Radic Biol Med 2017;105:41–47.
11. Stenke E, Bourke B, Knaus UG. NAPDH oxidases in inflammatory bowel disease. Methods Mol Biol 2019;1982:695–713.
12. Szanto I, Rubbia-Brandt L, Kiss P, Steger K, Banfi B, Kovari E, Herrmann F, Hadengue A, Krause KH. Expression of NOX1, a superoxide-generating NADPH oxidase, in colon cancer and inflammatory bowel disease. J Pathol 2005;207:164–176.
13. Kim JS, Diebold BA, Babior BM, Knaus UG, Bokoch GM. Regulation of Nox1 activity via protein kinase A-mediated phosphorylation of NoxA1 and 14-3-3 binding. J Biol Chem 2007;282:34787–34800.
14. Kroviarski Y, Debbabi M, Bachoual R, Périanin A, Gougerot-Pocidalo MA, El-Benna J, Dang PM. Phosphorylation of NADPH oxidase activator 1 (NOXA1) on serine 282 by MAP kinases and on serine 172 by protein kinase C and protein kinase A prevents NOX1 hyperactivation. FASEB J 2010;24:2077–2092.
15. Debbabi M, Kroviarski Y, Bournier O, Gougerot-Pocidalo MA, El-Benna J, Dang PM. NOXO1 phosphorylation on serine 154 is critical for optimal NADPH oxidase 1 assembly and activation. FASEB J 2013;27:1733–1748.
16. Yamamoto A, Takeya R, Matsumoto M, Nakayama KI, Sumimoto H. Phosphorylation of Noxo1 at threonine 341 regulates its interaction with Noxa1 and the superoxide-producing activity of Nox1. FEBS J 2013;280:5145–5159.
17. Litchfield DW. Protein kinase CK2: structure, regulation and role in cellular decisions of life and death. Biochem J 2003;369:1–15.
18. St-Denis NA, Litchfield DW. Protein kinase CK2 in health and disease: from birth to death—the role of protein kinase CK2 in the regulation of cell proliferation and survival. Cell Mol Life Sci 2009;66:1817–1829.
19. Koch S, Capaldo CT, Hilgarth RS, Fournier B, Parkos CA, Nusrat A. Protein kinase CK2 is a critical regulator of epithelial homeostasis in chronic intestinal inflammation. Mucosal Immunol 2013;6:136–145.
20. Yang W, Gibson SA, Yan Z, Wei H, Tao J, Sha B, Qin H, Benveniste EN. Protein kinase 2 (CK2) controls CD4+ T cell effector function in the pathogenesis of colitis. Mucosal Immunol 2020;13:788–798.
21. Raju P, Shashikanth N, Tsai PY, Pongkorpsakol P, Chanez-Paredes S, Steinhagen PR, Kuo WT, Singh G, Tsukita S, Turner JR. Inactivation of paracellular cation-selective claudin-2 channels attenuates immune-mediated experimental colitis in mice. J Clin Invest 2020;24:138697.
22. Cozza G, Pinna LA, Moro S. Protein kinase CK2 inhibitors: a patent review. Expert Opin Ther Pat 2012;22:1081–1097.
23. Zien P, Duncan JS, Skierski J, Bretner M, Litchfield DW, Shugar D. Tetrabromobenzotriazole (TBBt) and tetrabromobenzimidazole (TBBz) as selective inhibitors of protein kinase CK2: evaluation of their effects on cells and different molecular forms of human CK2. Biochim Biophys Acta 2005;1754:271–280.
24. Antoniou E, Margonis GA, Angelou A, Pikouli A, Argiri P, Karavokyros I, Papalois A, Pikoulis E. The TNBS-induced colitis animal model: an overview. Ann Med Surg (Lond) 2016;11:9–15.
25. Wallace JL, MacNaughton WK, Morris GP, Beck PL. Inhibition of leukotriene synthesis markedly accelerates healing in a rat model of inflammatory bowel disease. Gastroenterology 1989;96:29–36.
26. Leroy D, Heriché JK, Filhol O, Chambaz EM, Cochet C. Binding of polyamines to an autonomous domain of the regulatory subunit of protein kinase CK2 induces a conformational change in the holoenzyme: a proposed role for the kinase stimulation. J Biol Chem 1997;272:20820–20827.
27. Ameho CK, Adjei AA, Harrison EK, Takeshita K, Morioka T, Arakaki Y, Ito E, Suzuki I, Kulkarni AD, Kawajiri A, Yamamoto S. Prophylactic effect of dietary glutamine supplementation on interleukin 8 and tumor necrosis factor α production in trinitrobenzene sulfonic acid induced colitis. Gut 1997;41:487–493.
28. Geiszt M, Lekstrom K, Witta J, Leto TL. Proteins homologous to p47phox and p67phox support superoxide production by NAD(P)H oxidase 1 in colon epithelial cells. J Biol Chem 2003;278:20006–20012.
29. Yokota H, Tsuzuki A, Shimada Y, Imai A, Utsumi D, Tsukahara T, Matsumoto M, Amagase K, Iwata K, Nakamura A, Yabe-Nishimura C, Kato S. NOX1/NADPH oxidase expressed in colonic macrophages contributes to the pathogenesis of colonic inflammation in trinitrobenzene sulfonic acid-induced murine colitis. J Pharmacol Exp Ther 2017;360:192–200, 27754929.
30. Ellson CD, Andrews S, Stephens LR, Hawkins PT. The PX domain: a new phosphoinositide-binding module. J Cell Sci 2002;115:1099–1105.

31. Wientjes FB, Reeves EP, Soskic V, Furthmayr H, Segal AW. The NADPH oxidase components p47(phox) and p40(phox) bind to moesin through their PX domain. Biochem Biophys Res Commun 2001;289:382–388.
32. D'Amore C, Salizzato V, Borgo C, Cesaro L, Pinna LA, Salvi M. A journey through the cytoskeleton with protein kinase CK2. Curr Protein Pept Sci 2019;20:547–562.
33. Meek DW, Simon S, Kikkawa U, Eckhart W. The p53 tumour suppressor protein is phosphorylated at serine 389 by casein kinase II. EMBO J 1990;9:3253–3260.
34. Vilk G, Weber JE, Turowec JP, Duncan JS, Wu C, Derksen DR, Zien P, Sarno S, Donella-Deana A, Lajoie G, Pinna LA, Li SS, Litchfield DW. Protein kinase CK2 catalyzes tyrosine phosphorylation in mammalian cells. Cell Signal 2008;20:1942–1951.
35. Yamamoto A, Kami K, Takeya R, Sumimoto H. Interaction between the SH3 domains and C-terminal proline-rich region in NADPH oxidase organizer 1 (Noxo1). Biochem Biophys Res Commun 2007;352:560–565.
36. Dutta S, Rittinger K. Regulation of NOXO1 activity through reversible interactions with p22 and NOXA1. PLoS One 2010;4:e10478.
37. Nagahama K, Ogawa A, Shirane K, Shimomura Y, Sugimoto K, Mizoguchi A. Protein kinase C theta plays a fundamental role in different types of chronic colitis. Gastroenterology 2008;134:459–469.
38. Kim YS, Lee JH, Park JW, Bae YS. Regulation of protein kinase CKII by direct interaction with the C-terminal region of p47(phox). Biochem Biophys Res Commun 2001;286:87–93.
39. Park HS, Lee SM, Lee JH, Kim YS, Bae YS, Park JW. Phosphorylation of the leucocyte NADPH oxidase subunit p47(phox) by casein kinase 2: conformation-dependent phosphorylation and modulation of oxidase activity. Biochem J 2001;358:783–790.
40. Litchfield DW, Lozeman FJ, Cicirelli MF, Harrylock M, Ericsson LH, Piening CJ, Krebs EG. Phosphorylation of the beta subunit of casein kinase II in human A431 cells: identification of the autophosphorylation site and a site phosphorylated by p34cdc2. J Biol Chem 1991;266:20380–20389.
41. Chassaing B, Aitken JD, Malleshappa M, Vijay-Kumar M. Dextran sulfate sodium (DSS)-induced colitis in mice. Curr Protoc Immunol 2014;104:15–25, 1–15.25.14.

Received April 19, 2021. Accepted January 4, 2022.

Correspondence
Address correspondence to: Pham My-Chan Dang, PhD, INSERM U1149, Faculté de Médecine Xavier Bichat, 16 rue Henri Huchard, Paris F-75018, France. e-mail: my-chan.dang@inserm.fr; fax: 33-157-27-74-61.

Acknowledgments
The authors thank Dr Martine Torres for her editorial help, Dr Aurélie Sannier for help with the interpretation of the histologic images of the colon sections, Olivier Thibaudeau for preparation of the paraffin sections, Samira Benadda for confocal microscopy, Véronique Legros and Laurent Lignières for mass spectrometry experiments, and Dr Corinne Dupuy for the gift of DUOX2 and DUOXA2 plasmids. D.L. is a recipient from the China Scholarship Council.

CRediT Authorship Contributions
Dan Liu, PhD (Conceptualization: Equal; Formal analysis: Equal; Methodology: Equal; Writing – original draft: Equal; Performed the experiments: Lead)
Jean-Claude Marie, PhD (Conceptualization: Equal; Formal analysis: Equal; Methodology: Equal; Writing – original draft: Equal)
Anne-Laure Pelletier, MD, PhD (Resources: Equal; Writing – review & editing: Equal)
Zhuoyao Song, PhD student (Performed the experiments: Supporting)
Marwa Ben-Khemis, PhD (Performed the experiments: Equal)
Kaouthar Boudiaf, PhD (Performed the experiments: Supporting)
Coralie Pintard, Assistant Engineer (Performed the experiments: Supporting)
Thibaut Leger, PhD (Formal analysis: Equal; Methodology: Equal; Validation: Equal)
Samuel Terrier, Engineer (Formal analysis: Supporting; Methodology: Equal; Validation: Supporting)
Guillaume Chevreux, PhD (Formal analysis: Equal; Methodology: Equal; Validation: Equal; Writing – original draft: Equal)
Jamel El-Benna, PhD (Conceptualization: Equal; Formal analysis: Equal; Methodology: Equal; Writing – original draft: Equal)
Pham My-Chan Dang, PhD (Conceptualization: Lead; Formal analysis: Equal; Funding acquisition: Lead; Methodology: Equal; Supervision: Lead; Writing – original draft: Lead)

Conflicts of interest
The authors disclose no conflicts.

Funding
Supported by La Ligue Nationale Contre le Cancer, Comité De Paris, grant no. RS18/75-13, INSERM, Labex Inflamex, CNRS and University of Paris.